MARIA S.MERIAN - Berichte

Variability and Trends in Physical and Biogeochemical Parameters of the Mediterranean Sea

Cruise No. MSM72

02.03.2018 – 03.04.2018,
Iraklion (Greece) – Cádiz (Spain)
MED-SHIP2

M. Álvarez, B. Astray, G. Bachi, V. Cardin, P. Celentano, S. Chaikakis, M.M. Chaves Montero, G. Civitarese, A. El Rahman Hassoun, N.M. Fajar, F. Fripiat, L. Gerke, A. Gogou, F. Guallart, B. Gülk, D. Hainbucher, N. Lange, A. Rochner, C. Santinelli, K. Schroeder,T. Steinhoff, T. Tanhua, L. Urbini, D. Velaoras, F. Wolf, A. Welsch

Dagmar Hainbucher
Institut für Meereskunde der Universität Hamburg

2019

Table of Contents

1 Cruise Summary

1.1 Summary in English

The last few decades have seen dramatic changes in the hydrography and biogeochemistry of the Mediterranean Sea. The complex bathymetry, the highly variable spatial and temporal scales of atmospheric forcing and internal processes contribute to generate complex and unsteady circulation patterns and significant variability in biogeochemical systems. Part of this variability can be influenced by anthropogenic contributions. Consequently, there is a need to document its details as well as to understand ongoing trends in order to better relate the observed processes and to possibly predict the consequences of these changes. The main goal of the cruise was to contribute to the understanding of long-term changes and trends in physical and biogeochemical parameters, such as the anthropogenic carbon uptake and to still evaluate the hydrographical situation after the major climatological shifts in the eastern and western part of the basin, known as the Eastern and Western Mediterranean Transients.

During the cruise, multidisciplinary measurements were conducted on a mainly zonal section along the whole Mediterranean Sea, contributing to the global repeat hydrography program GO-SHIP and adhering to the GO-SHIP requirements.

1.2 Zusammenfassung

In den letzten Jahrzehnten haben tiefgreifende Veränderungen in der Hydrographie und der Biogeochemie des Mittelmeers stattgefunden. Die komplexe Bathymetrie, die hohe räumliche und zeitliche Variabilität des atmosphärischen Antriebs und interne Prozesse tragen zu einem komplexen, instationären Zirkulationsmuster und einer signifikanten Variabilität des biogeochemischen Systems bei. Ein Teil dieser Variabilität kann durch anthropogene Beiträge beeinflusst werden. Daher ist es erforderlich, diese Details zu dokumentieren und die aktuellen Trends zu verstehen, um die beobachteten Prozesse zuzuordnen und die Auswirkungen der Änderungen vorhersagen zu können. Das wesentliche Ziel der Reise war, zum Verständnis von Langzeitänderungen und Trends in den physikalischen und biogeochemischen Parameter, wie der Aufnahme von anthropogenem Karbon, beizutragen und weiterhin die hydrographische Situation nach den wesentlichen Klimaverschiebungen im östlichen und westlichen Becken, die als der „Eastern und Western Mediterranean Transients“ bekannt wurden, zu bewerten.

Auf der Reise wurden multidisziplinäre Messungen auf einem im Wesentlichen zonalen Schnitt durch das gesamte Mittelmeer durchgeführt. Die Reise trägt zum globalen „repeat hydrography program“ GO-SHIP unter Berücksichtigung der GO-SHIP Anforderungen bei.

2 Participants

2.1 Principal Investigators

Name	Institution
Hainbucher, Dagmar	IfMHH
Tanhua, Toste	GEOMAR
Cardin, Vanessa	OGS
Civitarese, Giuseppe	OGS
Álvarez, Marta	IEO
Gogou, Alexandra	HCMR
Schroeder, Katrin	ISMAR
Chiara Santinelli	CNR-P
François Fripiat	MPI-M

2.2 Scientific Party

Name	Discipline	Institution
Dagmar Hainbucher	Chief Scientist	IfMHH
Vanessa Cardin	CTD/lADCP/uCTD/ADCP/Thermosal	OGS
Maria del Mar Chavez Montero	CTD/lADCP/uCTD/ADCP/Thermosal	OGS
Dimitrios Velaoras	CTD/lADCP/uCTD/ADCP/Thermosal	HCMR
Paolo Celentano	CTD/lADCP/uCTD/ADCP/Thermosal	ISMAR
Birte Gülk	CTD/lADCP/uCTD/ADCP/Thermosal	IfMHH
Andrea Rochner	CTD/lADCP/uCTD/ADCP/Thermosal	IfMHH
Andreas Welsch	Salinometer / technical support	IfMHH
Toste Tanhua	Transient tracers	GEOMAR
Fabian Wolf	Transient tracers	GEOMAR
Nico Lange	Transient tracers	GEOMAR
Lennart Gerke	Transient tracers	GEOMAR
Giuseppe Civitarese	Nutrients, TN, TP, Oxygen	OGS
Lidia Urbini	Nutrients, TN, TP, Oxygen	OGS
Spyros Chaikakis	LISST, POC, PON	HCMR
Noelia M. Fajar Gonzalez	Carbonate System	IEO
Elisa Fernández Guallart	Carbonate System	IEO
Blanca Astray Uceda	Carbonate System	IEO
Abed El Rahaman Hassoun	Carbonate System	CNRS-L
Giancarlo Bachi	DOC, CDOM	CNR-P

2.3 Participating Institutions

IfMHH: Institut für Meereskunde derUniversität Hamburg
GEOMAR: Helmholtz-Zentrum für Ozeanforschung, Kiel
OGS: Istituto Nazionale di Oceanografia e di Geofisica Sperimentale, Trieste, Italy
IEO: Instituto Español de Oceanografía (IEO), centro de A Coruña, Spain,
MPI-M: Max-Planck-Institut für Chemie, Mainz

CNRS-L: National Council for Scientific Research in Lebanon. National Center for Marine Sciences
ISMAR: Istituto di Scienze Marine, Venezia
HCMR: Helenic Centre for Marine Research, Athens
CNR-P: CNR Istituto di Biofisica Unità Operativa di Pisa

3 Research Program

3.1 Aims of the Cruise

The principal scientific objective of the cruise was to add knowledge to the different scales and magnitudes of variability and trends in the circulation, hydrography, and biogeochemistry of the Mediterranean Sea. Key variables were measured in key regions in order to understand changes, the reason for occurrence, and the drivers. These ambitious aims, of course, cannot be reached by one cruise alone, but it requires an adequate amount of data distributed in space and time. Therefore, the cruise contributed to the documentation of the water property distribution of the Mediterranean Sea.

The following science questions were addressed:

1. What are the long-term changes and/or trends in physics and biochemistry in the Mediterranean Sea, including all the sub-basins?
2. How is the hydrographic situation in the Mediterranean developing further on after the EMT and WMT? Is there still a trend of the system to return to the pre-EMT situation and is there a similar trend in the WMed?
3. How are eddies distributed in the EMed and WMed during the cruise? Do they differ in the sub basins? To what extend is heat and salt transferred into the vertical by eddies in the WMed and EMed during the cruise?
4. What is the rate of uptake of the anthropogenic carbon in the Mediterranean and is this changing over time?
5. What is the magnitude of variability and trends in the inventory of biogechemical variables (including oxygen and nutrients)?
6. What is the base-line values of rarely measured Essential Ocean Variables (EOVs) such as DOC and N_2O

3.2 Agenda of the Cruise

We carried out measurements of current and along-track hydrographic and biogeochemical variables with the classical instrumentation of CTD, lADCP, uCTD and bottle samples on highly resolved sections through the Mediterranean Sea. The high resolution of CTD stations, enhanced for the physical parameters by additional uCTD measurements, allowed us to resolve the eddy field on the sections. The recognition of the eddy field was also supported and complemented by satellite data.

Most of the sections and CTD-positions are repeat occupations (cruise M84 and other) in order to allow long term trend analyses. Along the different sections, CTD stations including sampling of chemical parameters were conducted approximately every 30 nm, CTD without sampling about every 15-20 nm and with even smaller spacing in the Straits. Between CTD stations underway CTD measurements were carried out and ADCP measurements were continuously conducted.

The water sampling program included measurements of all level 1 variables as defined by GO-SHIP (i.e. oxygen, macro-nutrients, transient tracers and the carbonate system) and measurements of the biogeochemical EOVs ^{13}C, N_2O and dissolved organic carbon (DOC). These data were used to quantify trends and variability of ventilation and biogeochemical cycles, in particular uptake of anthropogenic carbon.

3.2 Description of the Work Area

The main focus of this cruise lied on an east-west transect through the Western and Eastern Mediterranean Sea (figure 3.2.1) starting east of Crete and ending close to the Strait of Gibraltar which is a repeat hydrography line in GO-SHIP (MED1). Primarily, it was planned to start the section east of Cyprus to measure the water masses originating from the Levantine basin. Diplomatic permissions were therefore applied for this region from the Greek as well from the Turkish administrations. Although permissions were granted from both sides, the different interpretation of the right to claim this region made it impossible for us to carry out our measurements at that moment without risking some diplomatic implication. So, we resigned to go there.

Cross sections through the important passages, the Strait of Otranto, Kasos Strait, Antikithera Strait, Strait of Sicily and Strait of Gibraltar were additionally conducted in order to characterize the inflow and outflow fluxes. Through the eastern Ionian Sea CTD stations were carried out to quantify Levantine Surface Water (LSW) fluxes to the Adriatic Sea and to trace the outflow of Adriatic Deep Water (AdDW) into the Ionian.

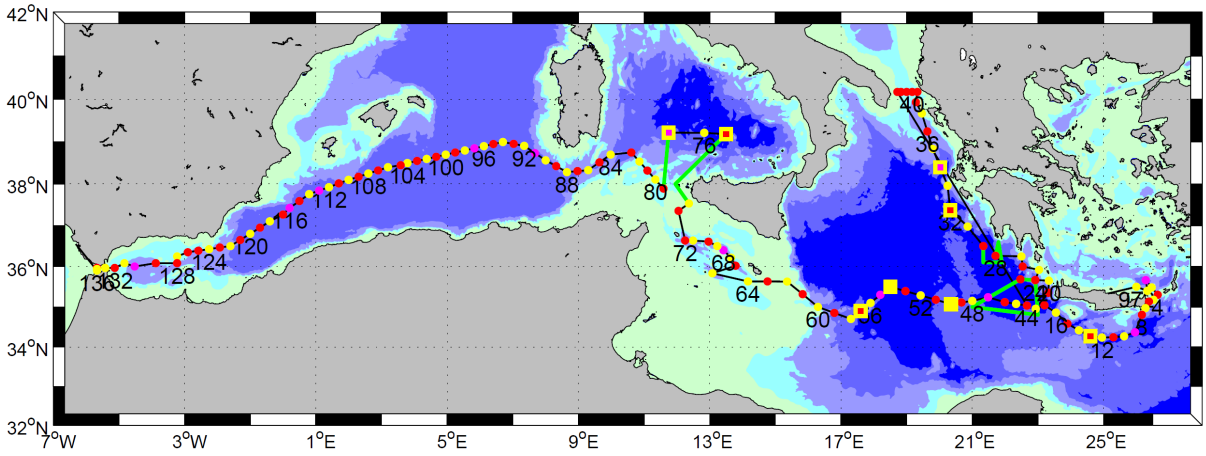

Fig. 3.2.1 Station Map. Yellow dots: CTD without any chemical sampling, red dots: CTD with chemical sampling, pink dots: CTD with chemical and additional sampling of isotopes, yellow squares: deployment of drifter and floats, green lines: fine resolved uCTD and ADCP tracks. Black lines: Track with uCTD casts between CTD stations.

4 Narrative of the Cruise

The scientific crew embarked at around 9:00 am on March 1st. The ship then left the port of Heraklion at 9:30 in the evening to bunker fuel in Kali Limenes the next morning. In the early afternoon of March 2nd we finally started our transfer to our first CTD station in the coastal area northeast of Crete. Unfortunately, this was not the first station we planned for the cruise. In view of the territorial ambiguities in parts of the work area, which only became clear shortly before the start of the cruise, the station plan was modified and adapted and we cancelled all stations east of our new first station.

During transfer and during bunkering we already unpacked our equipment and started to install the instruments. However, some of us had to stay in bed because of a cold with a feverish course. We received our mandatory safety briefing shortly after embarking and a safety exercise on the next day in which we also had to board the lifeboat. Everything went well and the scientific crew started to feel comfortable on board. On March 2nd at 10:30 pm we began with the station work. We started with CTD stations north-east of Crete in the Aegean Sea, carried out CTD stations in the Strait of Kasos, and then moved south of Crete to the west into the Ionian Basin. Along the Strait of Antikythera we steamed northwards in the height of the Peloponnese. Our main program was taking CTD casts. Here, the biogeochemists took water samples from several depths to determine different parameters (nutrients, oxygen, inorganic carbon, etc.). We took biogeochemical samples in about every second station, because the laboratory analysis is sometimes very time-consuming. At a few stations, the CTD was run twice in order to cover the demand for water for additional biogeochemical measurements. The deepest CTD station was station 23 with 4528 m water depth which we reached on the 8th of March. From station 15 (5.03.2018 early morning) onwards, we additionally took underway CTD measurements between the CTD stations. During these measurements we reduced the ship's speed to about 3 knots, so we were able to reach depths between 600 - 800 m with the uCTD. On station 13 on 4th of March at around 20:30 UTC we deployed the first AVOR float and a surface drifter. After station 21 on the 7th of March early morning, we interrupted our CTD work in order to investigate eddies for the first time on our cruise with fine resolved measurements. For this purpose, the uCTD was run about every hour, the ship speed between the stations was about 8 nm, while during uCTD measurements it was reduced to 3 nm. The route was determined using maps of dynamic topographies. Another "eddy track" followed after station 28 on the 10th of March. On these sections we are especially interested in the continuous ship's ADCP measurements, which we hope will help us to recognize eddies also in their vertical extension. Our northernmost stations were in the Strait of Otranto which we reached on the 12th of March in the afternoon. The section through the Strait of Otranto is repeatedly taken on cruises by us, as the Adriatic Sea is the most important producer of deep water in the Ionian Basin and we are interested in the changes in the outflow of deep water over long time scales. After this northernmost section a long transit route followed back to our section across the Mediterranean Sea, which we resumed with station 44 on the 14th of March west of Crete. On the transit, we continued to continuously collect data with the ADCP and ran an uCTD approximately every two hours. Additionally, we had some time to visit the ship`s engine. On stations 50 (15.03.2018 23:30 UTC), 54 (16.03.2018, 20:00 UTC) and 56 (17.03.2018 07:30 UTC) surface drifters and additionally an AVOR float (station 56) were deployed. At station 34 (11.03.2018 23:00 UTC) we dropped the only PROVOR BIO float.

Unfortunately, we had to contend with considerable technical problems with the CTD. On Monday, March 6 at 22:00, station 18, the rosette returned on deck with 2 missing and 3 broken Niskin bottles. First of all, we suspected an operating error when clamping one or more bottles. But then the release unit also stopped working. From now on, none of the bottles could be closed electronically in the water. So we swapped plugs, cables and devices. We first drove our own CTD and rosette and finally the CTD and rosette of the ship. But nothing helped. We also exchanged the winches. It turned out that the errors were caused by the defective releaser unit of our rosette and by the termination of the winches. Communication with the release unit was interrupted during tension and movement. On the next station everything worked fine, but on

station 24 (09.03.2018 09:30 UTC) some of the bottles did not close again, and this time there were also faulty data transfers. We replaced the ship's CTD to its backup CTD. CTD operation ran then smoothly for some stations with the ship's own rosette and CTD. But on the evening of March 14, both oxygen sensors showed only noisy profiles from approx. 1000 m on, combined with a sudden offset. Now everything started again from the beginning, we exchanged cables, sensors and even the winches again. But all this did not help here either. Finally we decided to connect our CTD including sensors with the ship's own rosette. But for that we had to build an adapter cable, because the rosette of the ship uses different plugs (Subconn) than for our CTD (Seacon).

On the 15th of March 06:00 UTC, station 47, we placed our CTD in a deep sea brine pool on a depth of 3528 m. These brines contain hydrogen sulphide and the water samples brought along smell accordingly when they arrive on deck. The laboratories were ventilated long after the event. Probably we came across the "l'Atalante Basin".

The weather had declined since 17th of March. Again and again smaller strong wind events with up to 9Bft took place during which we had to suspend the uCTD work. However, the CTD stations could be carried out as planned. On Monday, 19.03.2018, we had a seminar in which we discussed the state of work and presented first results of the cruise. The next day we started a fine resolving ADCP track on the Sicily shelf. The area was too flat and the swell too high to take uCTD profiles additionally. Now that more than half of our cruise was over, we celebrated this in the evening of the same day. We entered the western basin of the Mediterranean Sea during the night to the 21st of March and had stations in the Tyrrhenian Sea. Again, on station 75 and 76, we were facing technical problems with the rosette but the problem was quickly solved. We deployed another float on Wednesday, 21.03.2018, after station 75 and continued also with uCTD measurements. On Thursday, 22.03.2018, we dropped the last ARGO float on this cruise on CTD station 77. At 8:00 in the morning on the same day we started another fine resolving uCTD/ADCP section to track eddies. The weather was mixed and we had to stop the uCTD measurements every now and then. The weather at the beginning of the last week of our cruise was windy with an average of 5 Bft, but allowed all work. We progressed quickly and according to plan. On Friday, 26.03., however, we had sunshine but winds up to 9 Bft, so the uCTD casts had to be discontinued again. On Saturday the weather calmed down again, the uCTD work was resumed and on Easter Sunday, April 1st, we could drive our last CTD station, No. 136, at calm sea in the Strait of Gibraltar, in the afternoon. We celebrated this with a little drink. After the station we set course to the port of Cádiz, where we arrived on Monday morning. After the last CTD, the continuous data acquisition of the ADCPs and the thermosalinograph were also completed on the transit. We started to dismantle our equipment, load the container and clean the laboratories. Due to the cancelled stations at the beginning of this cruise, we entered the port of Cádiz one day earlier than expected.

5 Technical Information and Preliminary Results

5.1 Physical Measurements

V. Cardin, P. Celentano, M. M. Chaves Montero, B. Gülk, A. Rochner, D. Velaoras, A. Welsch

The sampling during the MSM72 cruise can be divided in two main categories: *Stationary sampling* (CTD and lADCP stations) which required the ship to stop in order to deploy

instruments over the side and *Underway samplings* (thermosal, uADCP and VM-ADCP) which is carried out either continuously or discretely but does not require the ship to stop.

5.1.1 Stationary sampling

During MSM72 Cruise a total of 136 CTD-stations were used for the hydrographic, biogeochemical survey, for vertical current (lADCP system) and for calibration (uCTD probes vs CTD).

CTD Observations

Altogether 136 CTD cast were performed from which 18 catalogued as isotopic, 65 as chemical and 59 as physical. Only for the isotopic stations in most of the cases 2 cast were performed depending on the depth from which the first cast was a full profile one and the second a shallow. During the physical stations probes at 3 levels were taken for salinity analysis. The samples were analyzed on board using a Guildline Autosal Salinometer. The batch-no. of the standard seawater samples is 38H13 which have a K_{21} factor of 1.07550 (practical salinity = 37.987) for the Eastern Mediterranean and batch-no. P160 with a K_{21} factor of 0.99983 (practical salinity = 34.993) for the Western. A total of 162 samples in 59 stations were taken during the cruise. The offset with respect to standard water varied from 0.0002 to 0.0030 depending on the laboratory temperature.

The primary CTD system initially used on board was a Seabird SBE9plus + CTD s/n 0285 from the University of Hamburg connected to a SBE11 deck unit, configured with a 24- position SBE-32 pylon (from GEOMAR) with 10 liter Niskin bottles. Position of bottles #23 and #24 was occupied by the lADCP. Initially, the CTD was set up with two temperature sensors, two conductivity sensors, oxygen sensor, fluorometer and altimeter. One test station was performed on the Cretan Sea before starting the programed ones (Config #1-2). On March 5th during the lowering of the rosette on station 19, due to an electrical problem, 5 bottles closed and exploded. After a careful check it was established that the problem was due to a malfunction of the pylon of the rosette and not to human error. Rosette and CTD (including sensors) were changed for those in equipment to the ship (CTD #807) and a new configuration was set adding a second oxygen sensor and turbidity as well (Config. #3, stations #20 and #21). Due to the configuration of the new rosette the lADCP was installed instead of bottles #22 and #23. Both oxygen sensor values showed a negative offset if compared with those obtained with the Winkler method from the bottle samples, so they were replaced (config 4, stations #22 to #25). Other problems rose up so both CTD, seacable and other cables and connectors were changed with those further provided by the ship (config 5). On March 14th (Station # 44) both oxygen sensors showed jumps after reaching high depths. As the problem continued the oxygen sensors #1 and #2 were changed from Volts 0, 1 to 6, 7 in the configuration file (Config 6) in station 49. Other attempts were made by initially isolating oxygen sensor #2 (Config 7, station 50) and then #1 (Config 8, station 51). In order to understand if the problem resided in the pair of oxygen sensors only, these sensors were changed for those already used but with high offset (Config 9, station 52).

In the search for the problem, in station #53 the pumps were replaced with new ones so as the CTD main unit, but unfortunately they did not solve the problem (Config 10). A new cable was made so that the CTD of the University of Hamburg could be installed again and be compatible with the ship's rosette (Config 11, stations 58-75_1). In this case the second oxygen sensor was installed to the detriment of the fluorometer. A test for the Ship CTD # 806 was performed

during the second cast of Station #75 (Config # 12) and after it the system was changed again as to the previous one. Again problems rose since water entered to the self-made cable during the execution of the following station (Config #13), so it was decided to put back the ship CTD recently tested. A complete system configuration with sensors serial numbers and ownership used in each config is depicted in table 5.1.1.

Table 5.1.1 CTD configurations, applied to casts and used during the MSM72 cruise

Config #	ST.	CTD #	PRIMARY T/C SENSORS		SECONDARY T/C SENSORS		OXYGEN SENSORS				ROSETTE
			T	C	T	C	Ox1	Ox2	Fluo	Turb	
1	1	285 (H)	1717 (OGS)	3442 (OGS)	NO	NO	3392 (OGS)	1761 (H)	SeaPoint SCF2874	NO	(G)
2	2 - 19	285 (H)	1717 (OGS)	3442 (OGS)	1294 (H)	1106 (H)	3392 (OGS)	X	SeaPoint SCF2874	NO	(G)
3	20-21	807 (S)	5716 (S)	4152 (S)	5719 (S)	4159 (S)	2417 (S)	2418 (S)	WET LAB 1755	WET LAB 1755	(S)
4	22-25	807 (S)	5716 (S)	4152 (S)	5719 (S)	4159 (S)	0951 (S)	0881 (S)	WET LAB 1754	WET LAB 1754	(S)
5	26-48	806 (S)	5716 (S)	4152 (S)	5719 (S)	4159 (S)	0951 (S)	0881 (S)	WET LAB 1754	WET LAB 1754	(S)
6	49	806 (S)	5716 (S)	4152 (S)	5719 (S)	4159 (S)	0951 (S)	0881 (S)	WET LAB 1754	WET LAB 1754	(S)
7	50	806 (S)	5716 (S)	4152 (S)	5719 (S)	4159 (S)	0951 (S) dummy	0881 (S)	WET LAB 1754	WET LAB 1754	(S)
8	51	806 (S)	5716 (S)	4152 (S)	5719 (S)	4159 (S) dummy	0951 (S)	0881(S)	WET LAB 1754	WET LAB 1754	(S)
9	52	806 (S)	5716 (S)	4152 (S)	5719 (S)	4159 (S)	2417 (S)	2418 (S)	WET LAB 1754	WET LAB 1754	(S)
10	53-57	806 (S)	5716 (S)	4152 (S)	5719 (S)	4159 (S)	0951 (S)	0881 (S)	WET LAB 1754	WET LAB 1754	(S)
11	58-75_1	285 (H)	1717 (OGS)	3442 (OGS)	1294 (H)	1106 (H)	3392 (OGS)	1761 (H)	NO	NO	
12	75_2	806 (S)	5716 (S)	4152 (S)	5719 (S)	4159 (S)	2417 (S)	2418 (S)	WET LAB 1754	WET LAB 1754	(S)
13	76_1	285 (H)	1717 (OGS)	3442 (OGS)	1294 (H)	1106 (H)	3392 (OGS)	1761 (H)	WET LAB 1754	WET LAB 1754	(S)
14	77-	806 (S)	5716 (S)	4152 (S)	5719 (S)	4159 (S)	2417 (S)	2418 (S)	WET LAB 1754	WET LAB 1754	(S)

S – RV M. S. Merian H – Hamburg University G – GeoMAR
OGS – Istituto Nazionale di Oceanografia e di Geofisica Sperimentale

Temperature, salinity and pressure data were post-processed by applying Seabird software and MATLAB routines. At this stage, spikes were removed, 1 dbar averages calculated. A first attempt to assess the performance of the conductivity sensors installed on the CTD-Rosette was done by comparing the salinity data with the bottle samples analyzed with the salinometer (table 5.1.2). Overall accuracies are within expected range of salinity (0.003).

Table 5.1.2 Mean differences for CTD salinity and sampled salinity obtained for each conductivity sensor

Conductivity Sensor # (owner)	Mean Difference	Std
#3422 (OGS)	-0.003738	0.004396
#1106 (H)	-0.002673	0.004141
#4152 (S)	0.000577	0.004091
#4159 (S)	-0.000395	0.004076

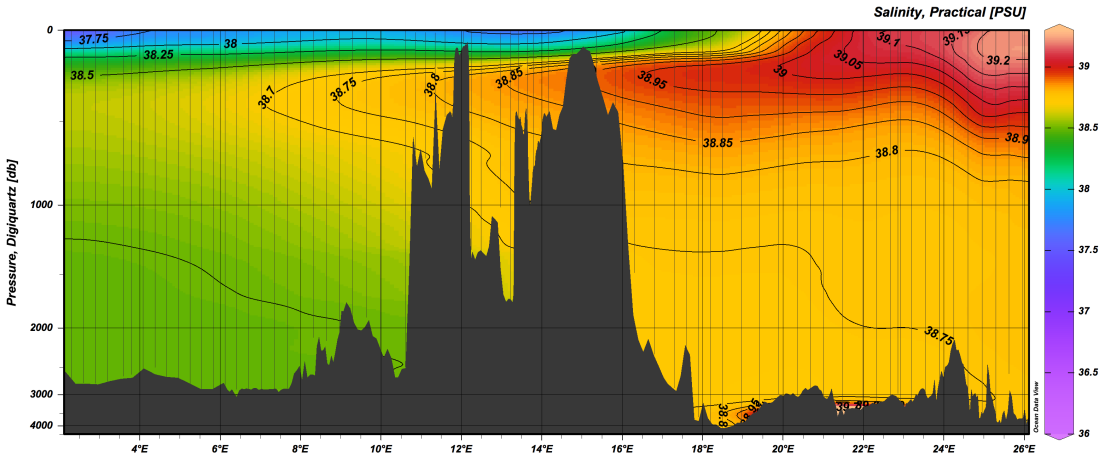

Figure 5.1.1

Fig. 5.1.1 Mediterranean West-East salinity transect showing the different salt content between both basins. A clearly intrusion of the salty Levantine Intermediate Water (LIW) from east to west in the first 500m is depicted while the low salinity Atlantic Water (AW) protrudes eastwards creating a front at about 20-22°E.

LADCP measurements

For measuring the ocean currents vertical profiles were made by a lADCP-2 system. The system uses two ADCPs of the Workhorse type (WHM300) manufactured by RD Instruments and operating at a frequency of 300 kHz. One of the ADCPs is looking upward (Slave s/n #22763) and the other one is looking downward (Master s/n #22762). During the cruise, the batteries of the lADCP were changed twice: The first time on the 17/03/2018 (Station 58) and the second time at the 27/03/2018 (Station 105). LADCP measurements were done at all CTD stations except for three (Station 73, 74, 80) with water depth less than 500 m. For these stations, the currents were observed by the ship mounted ADCP. At double stations / isotope stations profiles were only taken from the deep cast. The gained data were processed with LDEO Matlab LADCP-processing system Version 10.15 (Turnherr, 2014). This software uses the raw lADCP data, processed CTD data and navigational data from the CTD. The resulting data are the u- and v- velocities at the depth. The depth has a bin size of 8m.

For the top 1000m, the resulting velocities are looking reliable especially in comparison with the ships ADCP. Below 1000m, data is very noisy probably due to missing scatters. At station 67 (on the 19/03/2018), we tried a stop for a bottom track. Therefore, the rosette stopped roughly 60m above the ground for one minute to resolve the bottom currents better. At a first look, the results of the bottom velocities looked more promising than before. Therefore, we continued to stop for the bottom track. The processed data is used to investigate the velocities in Straits, for example Otranto Strait, or to gain information about the gyres (figure 5.1.2). The data is also compared with the ship ADCP data.

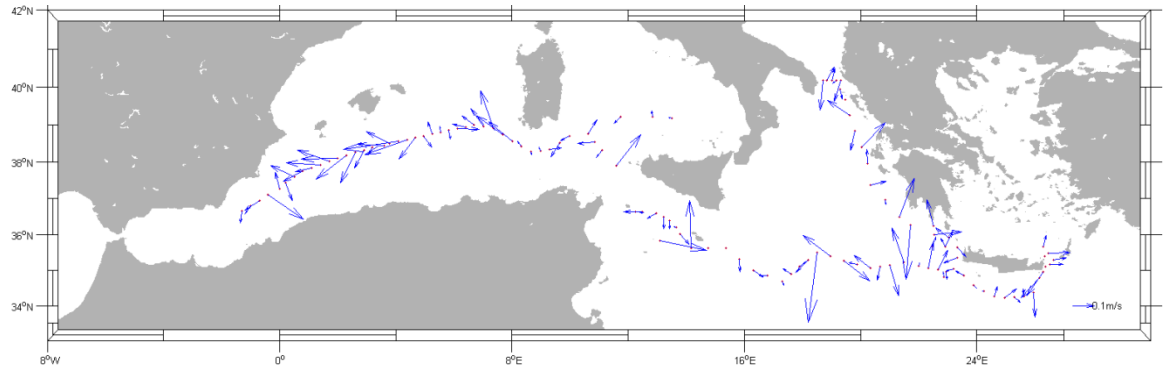

Fig. 5.1.2 Currents velocity at 400m for stations 1 to 121

5.1.2 Underway sampling

Thermosalinograph measurements

Underway temperature and salinity surface measurements were continuously acquired through two SeaBird thermosalinographs (TSGs, Container 2 and 3) installed in the ship's port well that alternate in active mode every six hours regularly; in standby mode the STG is cleaned. The vessel manages the switch and data acquisition.

For a preliminary data analysis onboard temperature, salinity, chlorophyll-a, turbidity data and metadata were daily extracted with a temporal resolution of 1 s. On March 9th, for unknown reasons, neither station was recorded for much of the day, creating a gap in the time series. Temperature and salinity measurements were validated and compared with the surface data of each CTD cast. In the visualization and further analysis, the data was averaged over 15 min intervals, so that spikes and fluctuations were removed. Overall surface temperature, salinity and chlorophyll-a concentration show reasonable values along the whole cruise. Surface temperature for almost the Mediterranean is depicted in figure 5.1.3. The two turbidity sensors, however, showed a constant offset of 0.7 NTU (TSG Container 2 measured turbidity values around 0.92 NTU and TSG Container 3 around 0.22 NTU). This finding is a known issue for the WTD (technical service of the ship), who observe a temporarily varying offset in the turbidity measurements for several months which could not be solved by a sensor calibration of the manufacturer. For calibration of the salinity measurement, water samples from the active TSG were taken approximately every 4 h, and then measured with the salinometer.

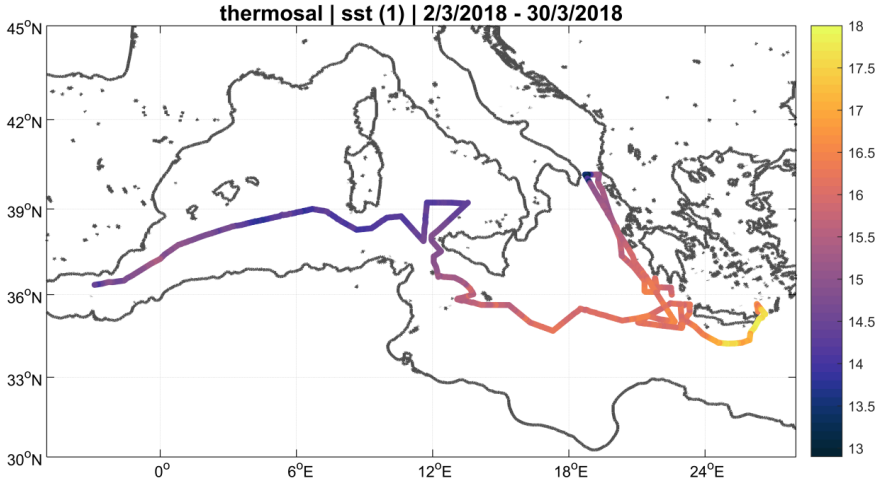

Fig. 5.1.3 Surface temperature recorded for both basins. Difference in temperature is depicted between the eastern and western Med.

During the cruise MSM-72, not only the water samples from this cruise are measured with the salinometer but also all TSG samples since 6th November (MSM-68/2), enabling us to detect trends and offsets over several months in the salinity measurements of the TSG. As a result both salinity sensors show an increasing offset from 0 to 0.04 psu (TSG measurement minus salinometer) between beginning of November 2017 until mid-March 2018 (figure 5.1.4). Furthermore, the spread of the calculated offsets increases for the samples from the Mediterranean Sea, i.e. for samples from MSM-71 and MSM-72 (after the 12th February); the standard deviation of the salinity differences between TSG and salinometer is ±0.0184 (±0.0153) outside the Mediterranean Sea and increases to ±0.0326 (±0.0343) in the Mediterranean for TSG Container 2 (Container 3). We are unable to determine the origin of this increased spread of the offsets. Our first idea was that the large spread emerged because the automatic correction by the salinometer software is not possible for samples having salinity as high as it is in the eastern Mediterranean Sea. However, in the western Mediterranean – during the second half of the cruise MSM-72 - the salinities are again low enough for an automatic correction, but the spread is still larger than before MSM-71. All these results were made available and discussed with the ship's system operators. Upcoming cruises will show if these trends continue in the future.

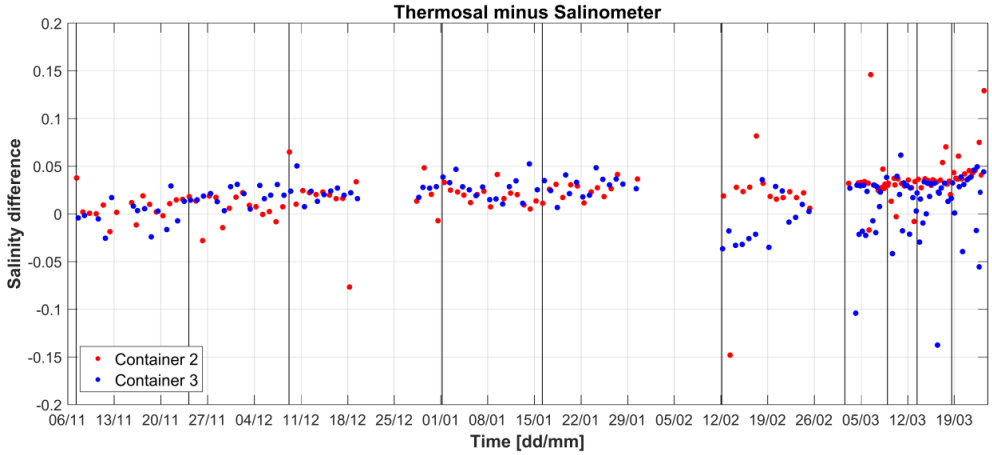

Fig. 5.1.4 Comparison between thermosal salinity and sampled salinity, the latter obtained from the salinometer analysis.

Current measurements with VM-ADCP

The hydrographic data set has been integrated with direct current measurements. During the whole campaign, underway current measurements were taken with two vessel-mounted VM-ADCPs Ocean Surveyor (ADCP) from RDI. The first, with work frequency of 75 kHz, cover approximately the top 500-700m of the water column. The number of bins was set to 100 with bin size of 8 m. The second, with work frequency of 38 kHz, has a depth range of about 1600 m, with the same bin number as the previous one and bin size of 16 m. Both instruments run in narrowband mode and were controlled by computers using the conventional RDI VMDAS software under a MS Windows system with a pinging set to fast as possible. No interferences with other used acoustical instruments were observed. The ADCP data was afterwards post-processed with the CODAS3 Software System, which allows extracting data, assigning coordinates, editing and correcting velocity data. Moreover, the data were corrected for errors in

the value of sound velocity in water, and misalignment of the instrument with respect to the axis of the ship (about -2.8 degrees for 75 kHz ADCP and about -0.15 degrees for 38 kHz ADCP).
Once the Netcdf data files were obtained from the CODAS software, it was necessary to apply the Matlab routines in order to get a definitive set of data for graphs. First, data corresponding to CTD stations were extracted and saved in .mat files, for any subsequent comparisons with the LADCP data. Then, the cleaned up ADCP data, were smoothed using a spatial average of Laplacians method. Finally, the desired transects were dug out, saved in ODV compatible files sections and were then plotted
Considering the route of the ship during the cruise, it was possible to identify different ADCP transects that correspond to areas with the most important water mass dynamics. In particular the most important sections were: gyre activity in the area west of Crete and south of Peloponnese, the west Cretan, Otranto (figure 5.1.5) and Sicily Straits, the east boundary of the Ionian Sea and the west-east Mediterranean transect.

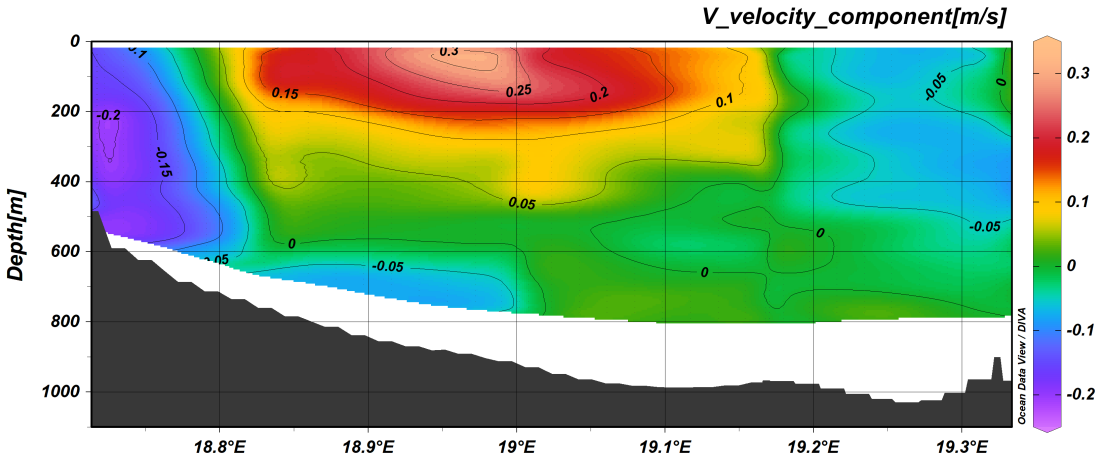

Fig. 5.1.5 Transect accross the Strait of Otranto from ADCP 38. The V-current component clearly shows the outflow of the Adriatic Deep Water (AdDW) along the eastern part while in the upper and intermediate layer of the central part the inflow of the Levantine Intermediate Water (LIW)

Underway Conductivity Temperature and Depth (uCTD)

Underway CTDs (uCTD) measurements provide high-resolution profiles of temperature, conductivity and depth, which allow characterizing upper ocean properties and identifying the position and characteristics of mesoscale structures. uCTD measurements were made with an Ocean Science uCTD system, winch S/N WI-0033. uCTD deployments did not require the ship to stop, but maintaining slower velocities during the deployments (around 3KN) is appropriate to reach larger depths.
The first uCTD deployment was done on the 5th of March, between CTD stations 015 and 016. After that, deployments were carried out between each CTD station in order to increase the sampling resolution. Several deployments were cancelled due to severe weather conditions. No uCTD was done when depth was shallower than 500m. Altogether 176 casts were taken with depths ranging from 557 to 864 m.
Two probes were used during the cruise, 183 and 289 (table 5.1.3). Deployments started with probe 289. In the first cast, the probe was configured to stop recording after 600 seconds, reaching 616 m depth. The configuration was changed to a no time limit mode after the second cast in order to get longer records. The probe tail spools were attached to the winch trough a rope

loop that was made new every day in the morning. Despite the probes can record several casts, data were downloaded right after each cast in order to avoid losing the data in case the probe was lost, and to free the memory. The probes were exchanged when the battery was running low (around 3.8V). On the 10th of March the 183 probe started showing problems during uploading of the data. Although no data were lost, afterwards the probe used for sampling was always 289, with the exception of cast 134 where probe 183 was used for calibration. In three occasions, no data were recorded. This occurred because the magnet was taken off twice before deployment. In case the magnet has to be removed, the advice is to wait some minutes before restarting the probe.

Protocol sheets were filled with deployment information (date, cast number, probe number, start lowering time, time of free fall, start heaving time, recovering time) and upload information (date, cast number, probe number, file name, ship velocity, maximum depth reached, battery voltage).

Table 5.1.3 Characteristics of the probes used during the cruise.

Probe	Device Type	Serial Number	Calibration date
0183	90745 uCTD / SBE 49 FastCat CTD	702-0183	12-Feb-2017
0289	90745 uCTD / SBE 49 FastCat CTD	702-0289	02-Nov-2016

For calibration purposes, some additional casts were done right after the CTD station in order to compare the data (table 5.1.4). The probes were also sent down with the starboard CTD in station 130.

Table 5.1.4 Characteristics of the probes used during the cruise.

CTD station #.	uCTD #.	Probe
21	7	289
71	110	289
85	122	289
88	126	289
94	134	183
100	142	289
106	150	289
112	158	289
115	162	289
118	167	289
121	170	289
129	173	289
130	176	183 and 289

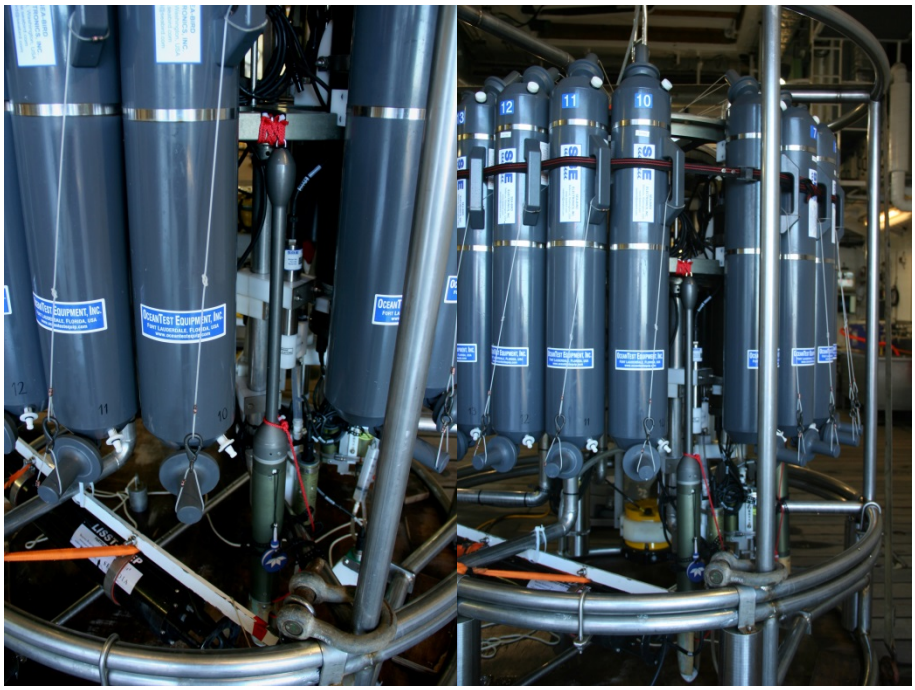

Fig. 5.1.6 *uCTD installed on the rosette during calibration cast.*

Data processing

The raw data were downloaded after each cast using the SBE software. Data collected in .asc files were processed using a set of matlab routines. After extracting the downcast data, a first correction was done for removing inaccuracies in the descend rate based on the work of Ullmann and Hebert (2013).

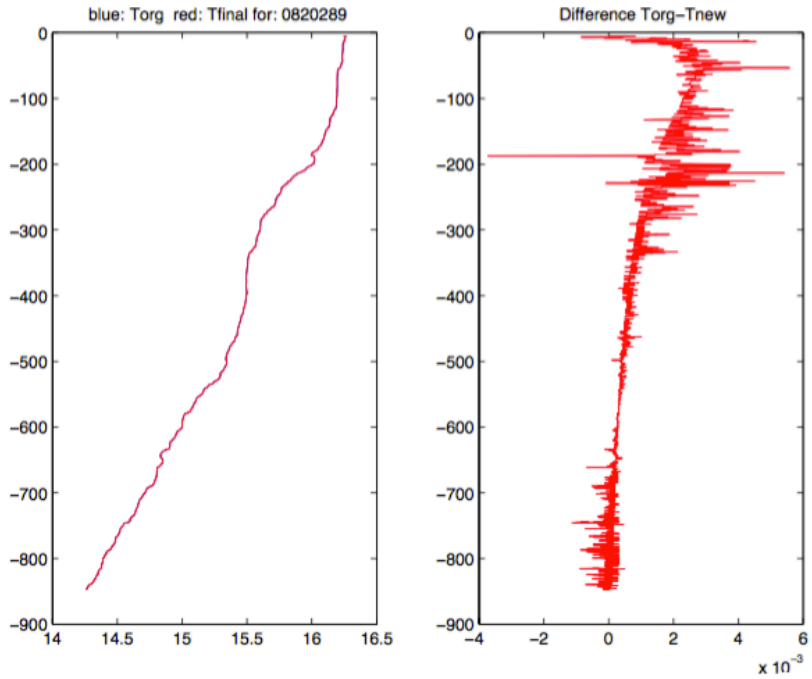

Fig. 5.1.7 uCTD cast corrected removing inaccuracies in the descend rate. A second correction will be done to eliminate errors due to different offsets of the uCTD probes compared to neighbor CTD profiles.

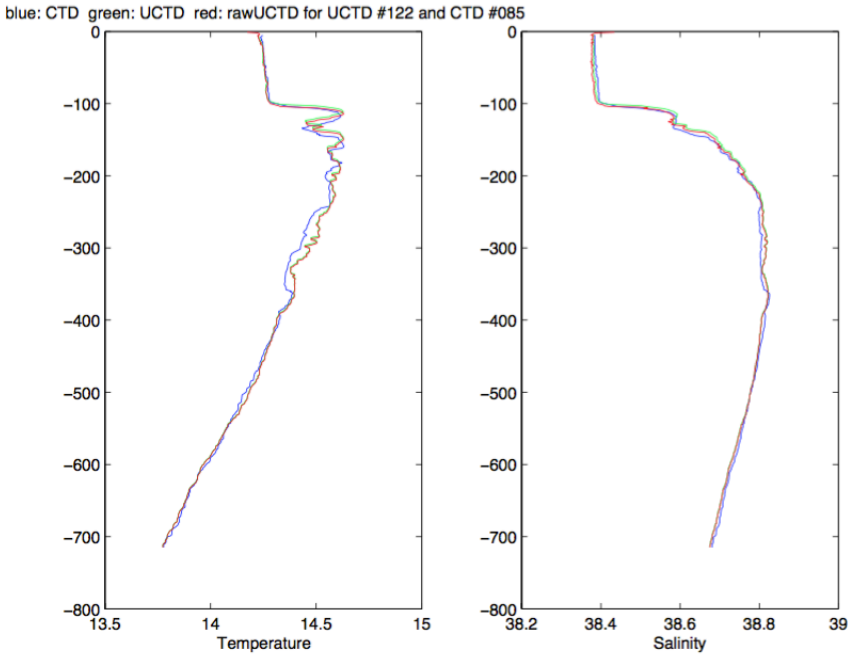

Fig. 5.1.8 Calibration performed using the most near-by CTD station.

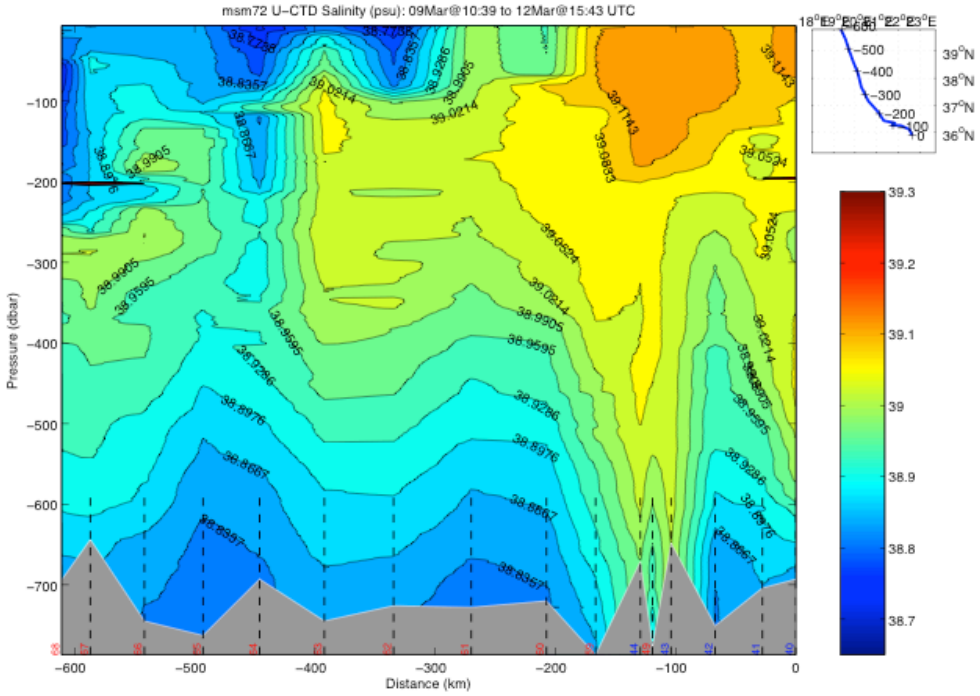

Fig. 5.1.9 uCTD salinity transect northward along the easternmost part of the Ionian Sea. Pelops gyre is well resolved around -100 Km.

5.2. Underway CO_2 and O_2 Measurements

(Tobias Steinhoff, Toste Tanhua)

Underway (UW) measurements of partial pressure of CO_2, and dissolved oxygen concentrations in seawater were carried out by means of a Contros HydroC pCO_2 analyzer for pCO_2 and an Aanderaa optode for oxygen.

The instruments were placed in a cooling box in the hangar (figure 5.2.1). Seawater was drawn from the ship's centrifugal pump for clean seawater that was continuously flowing through the cooling box with the inlet close to the instruments. Water was pumped through a SeaBird 5 salinity and temperature sensor and on to the HydroC instrument.
The system operated reliable during the whole cruise except that the data acquisition was interrupted for the pCO_2 instrument for 2 days, which was directly followed by the ship's centrifugal pump being turned off. This all resulted in a 5 day period without data between March 5 and 10.
During the cruise 13 samples were taken from the cooling box for discrete measurements of pH and total alkalinity.
The UW measurements started on March 2nd at 20:20 and stopped on April 1, 2018, at 14:00 (both UTC).

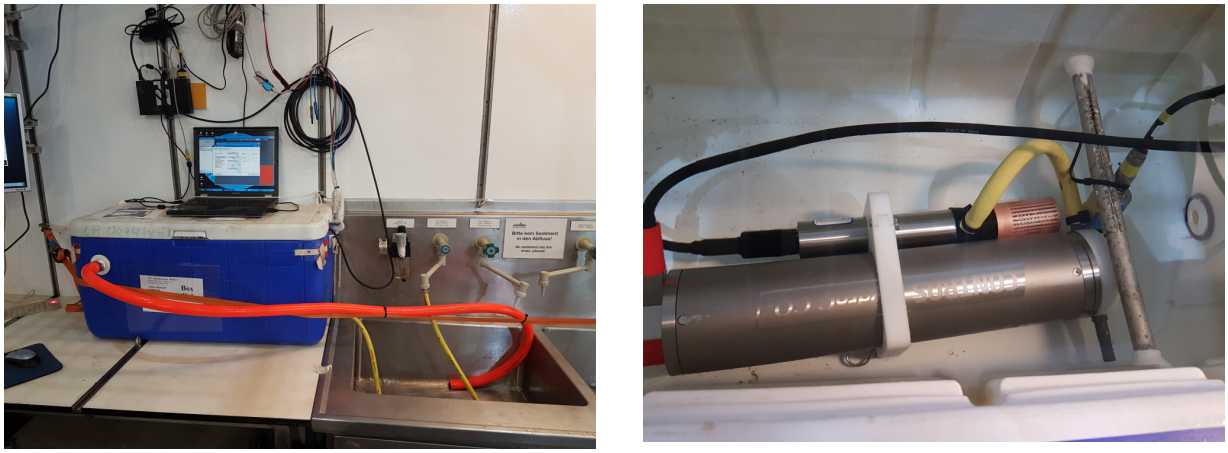

Fig. 5.2.1 Analytical set-up of the underway measurements during MSM72.

The underway oxygen measurements were calibrated by comparing to the Winkler measurements taken for surface samples at the CTD stations (figure 5.2.2).

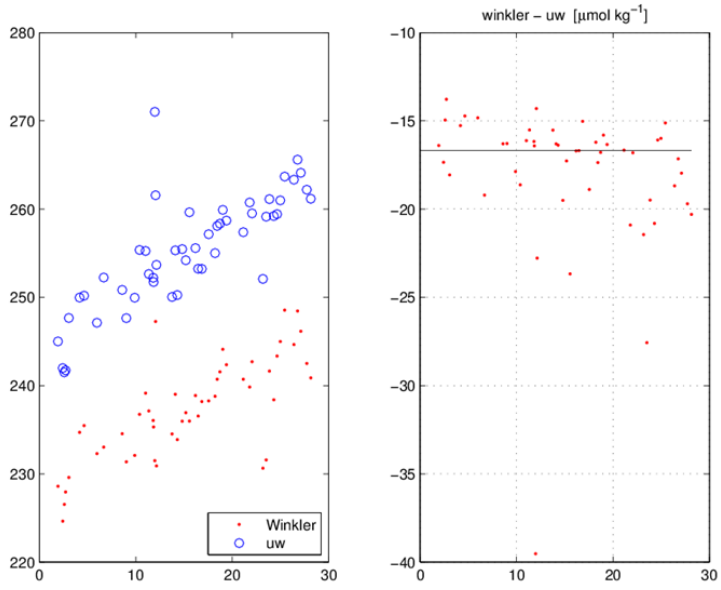

Fig. 5.2.2 Calibration of the underway oxygen optode data vs. winkler titrations of oxygen on CTD stations.

Preliminary results of surface pCO_2 (prior to post-cruise calibration of the sensor) are shown on Figure 5.2.3.

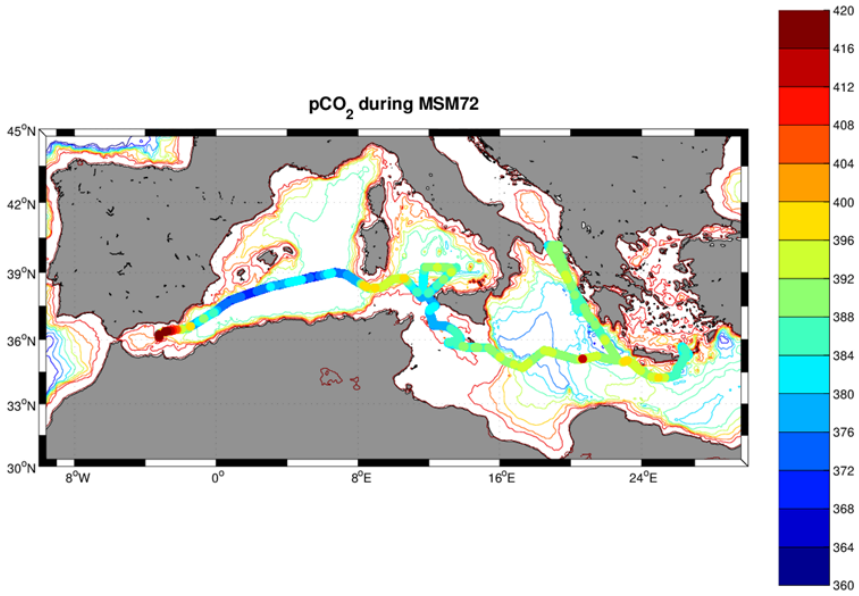

Fig.5.2.3 Surface pCO_2 distribution on cruise MSM72.

5.3 Dissolved Oxygen. (G. Civitarese, L. Urbini)

Dissolved oxygen in seawater was measured at every station and depth along the cruise and reported in µmol/kg. Oxygen was measured following the automatic Winkler potentiometric method modified after Langdon (2010). Titrations were done within the sampling calibrated flasks using an Automatic Titrator Mettler Toledo T50 (s/n 5129080332) with a platinum combined electrode.

Reagents blank and Thiosulphate standardisation were done daily by means of Potassium Iodate Standard 1.667 millimolar by OSIL, UK (Codes: 39004, 40082, 40078, and 39044).

About 1400 samples were analyzed on board during the cruise.

Precision

On board precision of dissolved oxygen measurements was determined on five replicates, at the beginning and at the end of the cruise. The results were:

Table 5.3.1 Precision of dissolved oxygen measurements.

Parameter	*Beginning of the cruise*			*End of the cruise*		
	Mean µM	STD µM	CV%	Mean µM	STD µM	CV%
DISSOLVED OXYGEN	196.07	0.13	0.07	198.84	0.14	0.07

In addition, during the cruise 46 duplicates were analysed. The results were:

Table 5.3.2 Precision of dissolved oxygen measurements by analyzing duplicates.

Parameter	Range µM	mean Absolute Difference (1) µM	mean Relative Percentage Difference (2)
DISSOLVED OXYGEN	179-240	0	0.09

*(1) AD=|duplicate #1 – duplicate #2|; (2) RPD%=Absolute Difference *100/mean (dupl. #1, #2).*

Preliminary results

The vertical distribution of dissolved oxygen along a section from the Cretan Sea to Sicily Channel, including part of the Cretan Passage and the southern Ionian is shown in Fig. 5.3.1. Oxygen Minimum Layer (<180 µmoles/kg) occupies the layer 500-1500m. Below, the western part of the Ionian appears more oxygenated than the eastern one due to the spreading of oxygenated Adriatic Dense Water from the Otranto Strait.

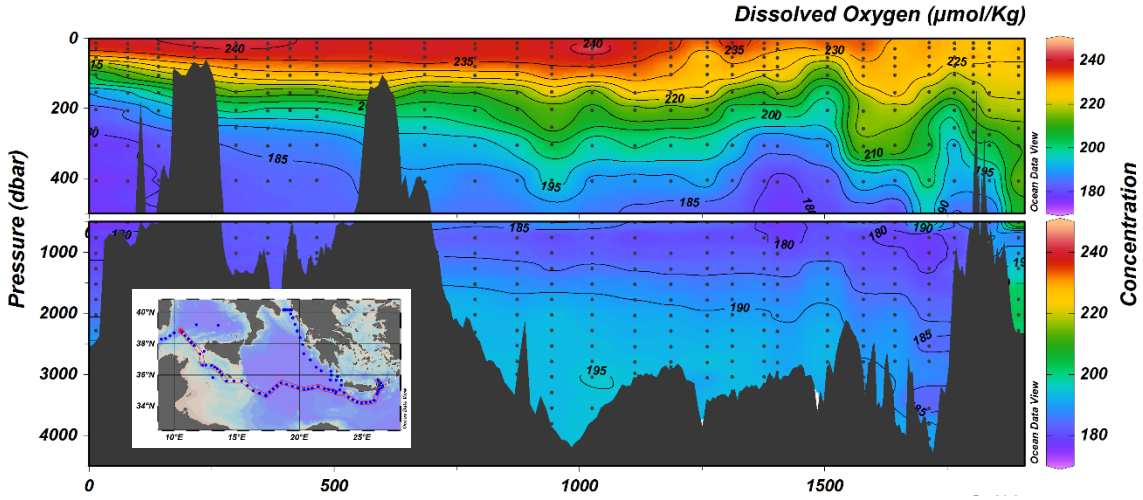

Fig. 5.3.1 Distribution of dissolved oxygen along a section from Cretan Sea to Sicily Channel.

5.4. Nutrients (nitrite, nitrate, phosphate, and silicate), Dissolved Organic Nitrogen (DON) and Phosphorus (DOP).

(L. Urbini and G. Civitarese)

Nutrients

Nutrients (nitrite, nitrate, silicate, and phosphate) were measured on-board by means of a QuAAtro auto-analyzer from SEAL analytics (s/n 8014549). The following protocols from SEAL analytics were followed:

Nitrite – (Method No. Q-030-04 Rev. 2)

Nitrie reacts under acic conditions with sulfanilamide to form a diazo compound that then couples with N-1-naphthylethylenediamine dihydrochloride (NEDD) to form a reddish-purple azo dye measured at 520 nm.

Nitrite and Nitrate – (Method No. Q-035-04 Rev. 4)

In the automated procedure for the determination of nitrate and nitrite, nitrate is reduced to nitrite at pH 8 in a copperized cadmium reduction coil. The nitrite reduced from nitrate plus any nitrite is transformed to a diazo compound that then couples with N-1-naphthylethylenediamine dihydrochloride (NEDD) to form a reddish.

Phosphate – (Method No. Q-031-04 Rev. 1)
The blue color is formed by the reaction of phosphate, molybdate ion and antimony ion followed by reduction with ascorbic acid. The reduced blue phospho-molybdenum complex is read at 880 nm.
Silicate – (Method No. Q-038-04 Rev. 0)
The procedure is based on the reduction of a silicomolybdate complex in acid solution to molybdenum blue by ascorbic acid. Oxalic acid is added to minimize interference from phosphate. The absorbance is measured at 820 nm.
About 1400 samples were analyzed on board.

Fig. 5.4.1 QuAAtro auto-analyzer from SEAL analytics.

Precision

Nutrient standardisation and data quality were assured through successful and continuous participation in international inter-calibration exercises.
The on board precision of nutrient measurements was determined on five replicates, at the beginning and at the end of the cruise. The results were:

Table 5.4.1 Precision of nutrient measurements.

Parameter	*Beginning of the cruise*			*End of the cruise*		
	Mean µM	STD µM	CV%	Mean µM	STD µM	CV%
NITRITE (1)	0.01	0.01	100	0.03	0.01	56.5
NITRITE + NITRATE	4.94	0.01	0.2	9.01	0.02	0.2
PHOSPHATE	0	0.01	5.5	0.41	0.01	3.1
SILICATE	8.34	0.03	0.3	9.55	0.04	0.5

(1) Nitrite statistics is given just for completeness, since the concentration levels recorded were too low, often below the detection limit.

In addition, during the cruise 140 duplicates were analysed. The results were:

Table 5.4.2 Precision of nutrient measurements by analyzing duplicates.

Parameter	Range µM	mean Absolute Difference (1) µM	mean Relative Percentage Difference (2)
NITRITE (3)	0-0.19	0.01	48.77
NITRITE+NITRATE	0.33-9.86	0.02	0.42
PHOSPHATE	0-0.47	0.01	5.13
SILICATE	0.93-11.00	0.04	0.72

(1) *AD=|duplicate #1 – duplicate #2|;* (2) *RPD%=Absolute Difference *100/mean (dupl. #1, #2);* (3) *Nitrite statistics was given just for completeness, since the concentration levels recorded were too low, often below the detection limit*.

Internal quality check was daily performed during the cruise by means of analyses of QUASIMEME samples, that provided the following results (within the already certified ranges):

Table 5.4.3 Precision of nutrient measurements by analyzing QUASIMEME samples.

Parameter	Certified Range µM	Mean µM	STD µM	CV%
NITRITE	0.46-0.51	0.51	0.01	2.1
NITRITE + NITRATE	6.43-7.08	6.92	0.1	1.4
PHOSPHATE	0.65-0.74	0.71	0.01	1.9
SILICATE	3.84-4.23	4.2	0.05	1.3

DON and DOP

About 550 samples for Dissolved Organic Nitrogen and Phosphorus (DON and DOP) analyses on land based laboratory were collected and frozen at -20°C after filtration on pre-combusted GF/F filter.

Preliminary results.

Fig. 5.42 provides the vertical distribution of nitrate along the section from Cretan Sea to Sicily Channel. Some remarkable features are: the maximum nutrient layer in the range of depth of 500-1500 m; the deepest layer showing an homogeneous distribution of nutrient; the nutrient impoverished upper layer, not yet completely depleted, subject to mesoscale dynamics (as, for example, south of Crete).

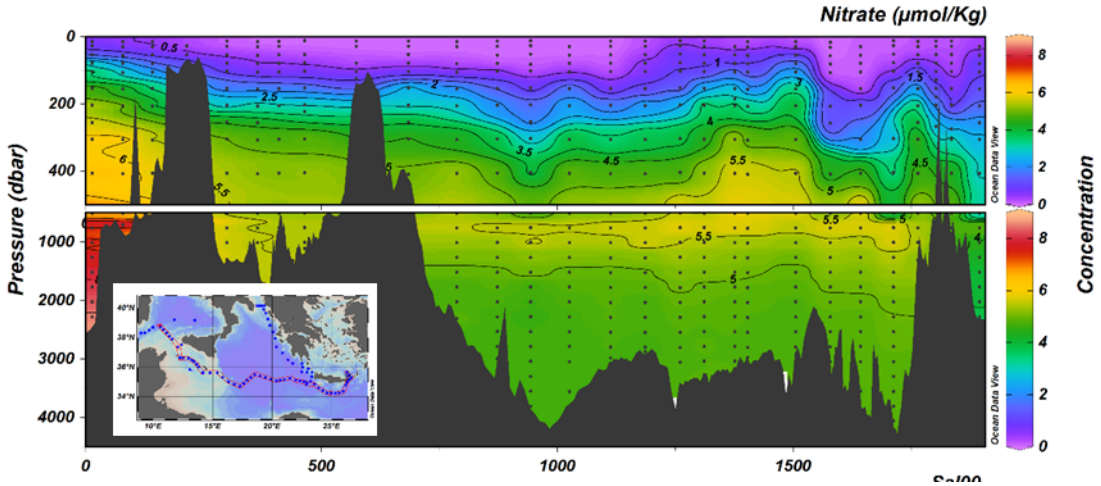

Fig. 5.4.2 Distribution of nitrate along a section from Cretan Sea to Sicily Channel.

5.5. CO_2 System

(Noelia M. Fajar; Elisa F. Guallart; Blanca Astray; Abed El Rahman Hassoun, Marta Álvarez)

The CO_2 variables sampled and measured on board the R/V Maria S. Merian were Dissolved Inorganic Carbon (DIC), pH, Total Alkalinity (TA) and ion carbonate (CO_3^{2-}). In addition, an underway partial pressure of CO_2 (pCO_2) CONTROS system was installed and surface samples for DIC, pH and TA were also analysed. The number of stations and samples analysed during the MSM72 cruise are summarized in table 5.5.1.

Table 5.5.1 Total number of stations and samples analysed during the MSM72 cruise.

MSM72	DIC	pH	TA	CO_3^{2-}	pCO_2
Stations	34	75	63	24	22
Samples	510	1431	991	421	-

5.5.1 Dissolved Inorganic Carbon (DIC)

DIC samples were analysed with a VINDTA 3D system (www.MARIANDA.com) (Figure 5.5.1), which briefly consists of extracting seawater CO_2 from the sample by adding phosphoric acid, followed by coulometric detection (Johnson et al., 1993).

Sampling

Seawater samples for DIC were collected after transient tracers and oxygen samples, in 500 ml borosilicate bottles. Samples were rinsed and filled smoothly from the bottom, overflowing the water by at least a half bottle volume. Samples were left at room temperature in the dark until analysis, maximum 3 days after sampling. Table 5.5.2 shows the selected stations for the DIC samples.

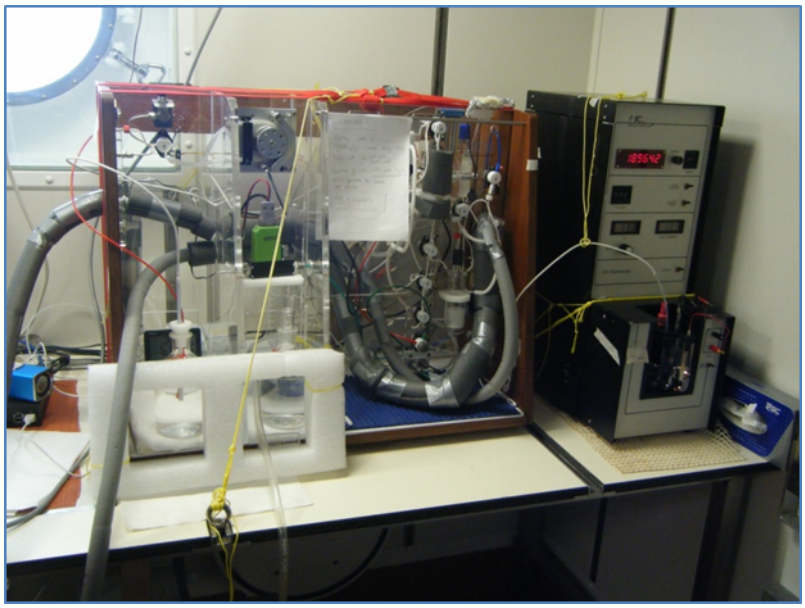

Fig. 5.5.1 VINDTA system at Trockenlabor in the R/V Maria S. Merian.

Analytical method

Samples for DIC were analysed with a VINDTA 3D coupled to a UIC 5011 coulometer. The VINDTA 3D 075 is designed by the company Marianda. The sample is kept at a constant temperature of 25°C with a cryostat bath (Polyscience). A calibrated volume of the sample (20 mL) is acidified with H_3PO_4 in a stripping chamber. The generated CO_2 is carried into a coulometer cell by a free-CO_2 gas, pure N_2, going through a condenser at a constant temperature of ~ 2°C. In the coulometer cell, the acid (hydroxyethylcarbamic acid) formed from the reaction of CO_2 and ethanolamine, is titrated coulometrically (electrolytic generation of OH^-) with photometric endpoint detection. The product of the time and the current passed through the cell during the titration (charge in Coulombs) is related by Faraday's constant to the number of moles of OH^- generated and, thus to the moles of CO_2 which reacted with ethanolamine to form the acid (Johnson et al., 1993).

The final value of DIC (µmol· kg^{-1}) is calculated using the following formula (Johnson et al, 1998):

$$\mathbf{DIC} = \frac{\mu\text{mol } C_{exp}}{\text{Titrated mass}}$$

Where:

$$\mu\text{mol } C_{exp} = (\text{Counts} - \text{Blank} \cdot \text{RT}) \cdot \frac{1\ \mu\text{mol C}}{4.82445 \cdot 10^3\ \text{counts}} \cdot \text{CALFACTOR}$$

Counts: counts from the coulometer.

Blank: mumber of counts in 10 min. Units: count/min

RT: run time.

Calfactor (calibration factor) the ratio of the theoretical CRM concentration and the experimentally obtained one

$$\textbf{Titrated mass} = \text{Corrected Volume (mL)} \cdot \text{Density (kg/mL)}$$

$$\text{Corrected Volume} = (((\text{Temp} - 20°\text{C}) \cdot 9.75 \cdot 10^{-6}) + 1) \cdot \text{Calibrated Pipette Volume referred to } 20°\text{C}$$

Faced Problems

The 2nd day of the MSM72 cruise, the Peltier cooler that keeps the condenser at 2°C broke down. We built a solenoid system around the condenser with a long and flexible rubber tube connected to a cryostat bath set at 2°C, keeping the condenser at a constant temperature (Figure 5.5.2). The samples were analysed at controlled room temperature of ~ 21°C (instead of 25°C) and the condenser was kept a constant temperature of 4°C (instead of 2°C) during the whole cruise. Apparently the different temperatures did not affect neither the precision nor the accuracy of the system.

Fig. 5.5.2 Home-made solenoid around the condenser to keep a constant temperature of ~ 2°C

Accuracy

No calibration unit neither gas loop are available for our VINDTA 3D. Therefore, no independent method to check the accuracy was available.

Certified Reference Material

In order to control the accuracy of DIC measurements, CO_2 Certified Reference Material (CRM) analyses were performed at the beginning and the end of every DIC batch of analysis. Those CRM were batch #158 (DIC = 2043.54 ± 0.46 µmol/kg) and batch #170 (DIC = 1982.42 ± 0.68 µmol/kg), provided by Prof. Andrew Dickson. Figures 5.5.3 and 5.5.4 show the CRM analysis for DIC, where the grey squares are the measured DIC values and the circles represent the mean value with the corresponding error bar per analysis session.

The CALFAC was calculated for each newly-prepared titration cell for each batch of analysis and gave the final DIC value. Small drifts or temporal biases were corrected, if necessary, by using the CRM sample at the end of the batch measurements.

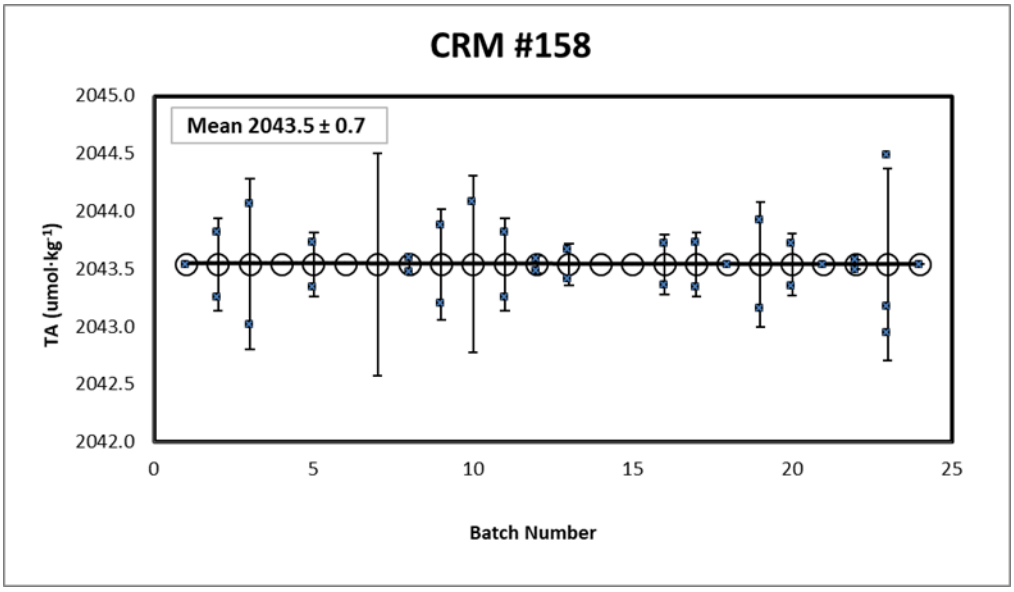

Fig. 5.5.3 DIC measurements of the CRM #158 during MSM72 at each analysis batch (batches 1-24).

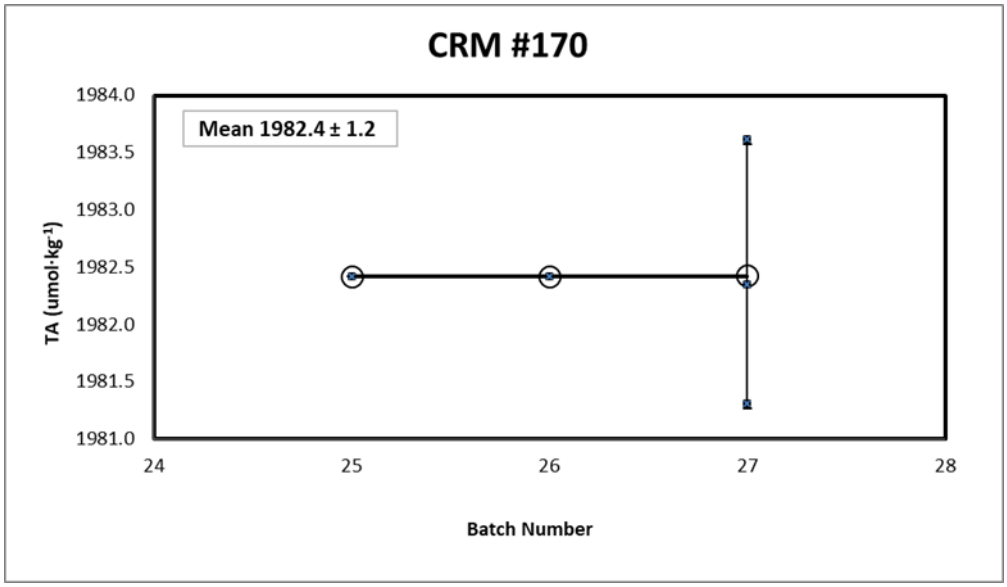

Fig. 5.5.4 DIC measurements of the CRM #170 during MSM72 at each analysis batch (batches 24-27).

Substandard

In addition, an extra control was conducted during the MSMS72 cruise by analysing a seawater substandard at the beginning and at the end of each batch of samples. This seawater substandard consisted of 700m seawater coinciding with the minimum salinity, stored in the dark into a large container (30L) at least 24h before its use. The repeated analysis of this water is the reference used to monitor the drift of the DIC measurements with time during the whole cruise. Those values are represented in Figure 5.5.5.

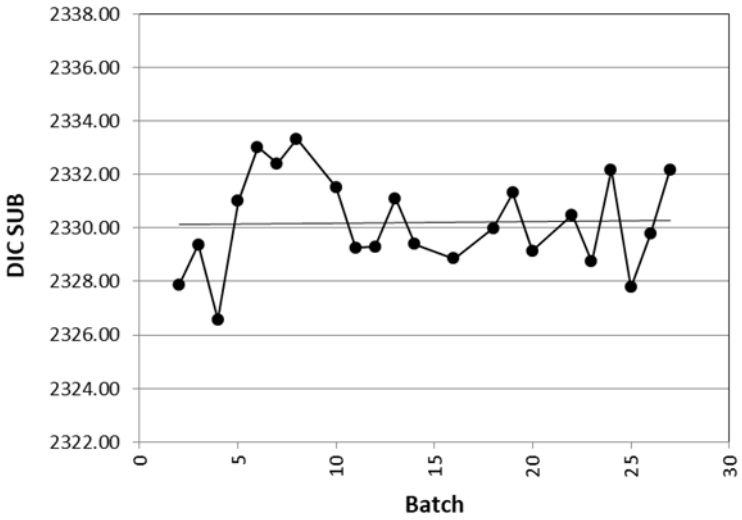

Fig. 5.5.5 DIC values for the substandard seawater represented against batch of analysis.

Table 5.5.2 Summarizes the information for each batch of analysis, including the calfactor, the mean DIC value for the CRM measurements, the mean value of the DIC measurements on the substandard samples and the average of the difference in the duplicate's analyses.

Batch	Counter	Date	Stations	Calfactor	Fitted DIC	Mean SUB DIC	Av.DIC Dif
1	16	03/03/2018	1, 2	1.004290	2043.54	2329.51	0.24 (4)
2	64	04/03/2018	2, 4,	1.004877	2043.54±0.40	2327.86±0.51	0.33 (5)
3	108	05/03/2018	8, 9,	1.004951	2043.54±0.74	2329.37±0.44	0.43 (2)
4	176	08/03/2018	13, 17	1.003840	2043.54	2326.57±0.52	0.73 (4)
5	220	09/03/2018	17	1.005178	2043.54±0.28	2331.01±1.01	0.51 (1)
6	270	10/03/2018	17, 23	1.004307	2043.54	2333.01±0.17	0.66 (5)
7	311	11/03/2018	23, 30,	1.003033	2043.54±0.96	2332.41±0.20	0.58 (3)
9	417	13/03/2018	34	1.004795	2043.54±0.48	2335.77±0.80	0.10 (2)
10	455	14/03/2018	38, 40,	1.004338	2043.54±0.77	2331.51±0.57	-
11	503	15/03/2018	40, 47,	1.002913	2043.54±0.40	2329.25±0.24	0.12 (1)
12	553	16/03/2018	40, 51, 52	1.001402	2043.54±0.07	2329.29±1.00	0.48 (5)
13	602	17/03/2018	51, 55	1.002278	2043.54±0	2331.11±0.58	0.62 (3)
14	648	18/03/2018	55, 56	1.002538	2043.54	2329.40±0.17	0.72 (2)
15	689	18/03/2018	59, 63	1.001384	2043.54	2324.85±0.47	0.52 (3)
16	733	19/03/2018	68	1.001563	2043.54±0.26	2328.85±0.70	0.60 (3)
17	774	20/03/2018	72	1.000340	2043.54±0.27	2324.56±0.07	0.54 (4)
18	822	22/03/2018	77	1.002945	2043.54	2329.99±0.41	0.45 (5)
19	890	23/03/2018	83	1.003781	2043.54±0.54	2331.31±0.77	0.13 (2)
20	946	24/03/2018	83, 87,	1.002515	2043.54±0.27	2329.14±0.52	0.53 (5)
21	998	25/03/2018	91	1.005194	2043.54	2336.78±0.88	0.00 (0)
22	1047	26/03/2018	97	1.001814	2043.54±0.04	2330.48±1.17	0.35 (4)
23	1103	27/03/2018	100, 102, 105	1.002474	2043.54±0.83	2329.47±1.03	0.93 (1)
24	1155	28/03/2018	105, 109	1.003669	2043.54	2332.17±1.13	0.55 (7)
25	1227	29/03/2018	109, 113	1.000191	1982.42	2327.78±1.14	0.45 (4)
26	1279	31/03/2018	113, 121	1.001296	1982.42	2329.77±0.13	0.59 (3)
27	1335	01/04/2018	130	1.000870	1982.42±1.15	2332±1.31	0.23 (2)

Precision

Five samples from the same Niskin bottle were taken to perform a typical reproducibility analysis at Western Basin (St 52 at bottom depth and St 56 at 100m) and Eastern Basin (St 100 at bottom depth and St 102 at 100m). Table 5.5.3 shows the mean DIC, the standard deviation and the number of analysed samples.

Table 5.5.3 Mean, standard deviation (STD) and number of cells collected from each Niskin at the different stations for the DIC analysis.

St	Salinity	Depth (m)	DIC (µmol/kg)	STD	n
52	38.727	3402.37	2309.50	0.63	5
56	38.605	103.56	2276.26	0.40	4
100	38.491	2764.03	2324.80	1.08	4
102	38.045	104.75	2262.21	0.91	5

In addition, consecutive duplicate analyses of the same sample were performed along the whole cruise each four or five samples. The mean standard deviation was 0.5 µmol Kg^{-1} (n=81). So, we consider the error of our DIC measurements lower that 1 µmol Kg^{-1}.

Results

The DIC results obtained during the cruise MSM72 are shown in figure 5.5.6. The upper panel show the DIC distribution along the Ionian Basin, while the lower panel show it along the longitudinal Eastern – Western basins, including the Cretan Waters.

5.5.2 pH

Spectrophotometric pH in seawater was measured following Clayton and Byrne (1993) at most of the chemical and isotope stations and at almost all depths during the MSM72 cruise. The pH is reported at 25°C on the Total scale (pH_{25T}).

Sampling

pH samples were taken immediately after DIC and directly from the Niskin bottles into cylindrical special optical glass Hellma cells of 28 mL of volume and 100 mm of path length, by overflowing the water and immediately sealing the cell. After sampling, the cells were carefully stored in an incubator, in which the temperature was controlled at 25 °C by the cryostatic bath around one hour before the analysis. Table 5.5.10 shows the selected stations for the pH samples (Sample Scheme section).

Analytical method

pH samples were measured using the fast, precise and commonly used spectrophotometric method described by Clayton and Byrne (1993). This method consists on adding a known volume of coloured indicator dye to the seawater sample and measuring the absorbance of the sample at controlled temperature of 25°C.

The indicator was a solution of m-cresol purple (Sigma Aldrich) prepared in seawater (2 mM) and maintained at dark, with no air contact.

All the absorbance measurements were obtained in the thermostatic (25 ± 0.2°C) cell compartment of the UV-Vis 2600 SHIMADZU double beam spectrophotometer. The temperature was controlled with a JULABO F12 ED (12L) cryostatic bath (Figure 5.5.7).

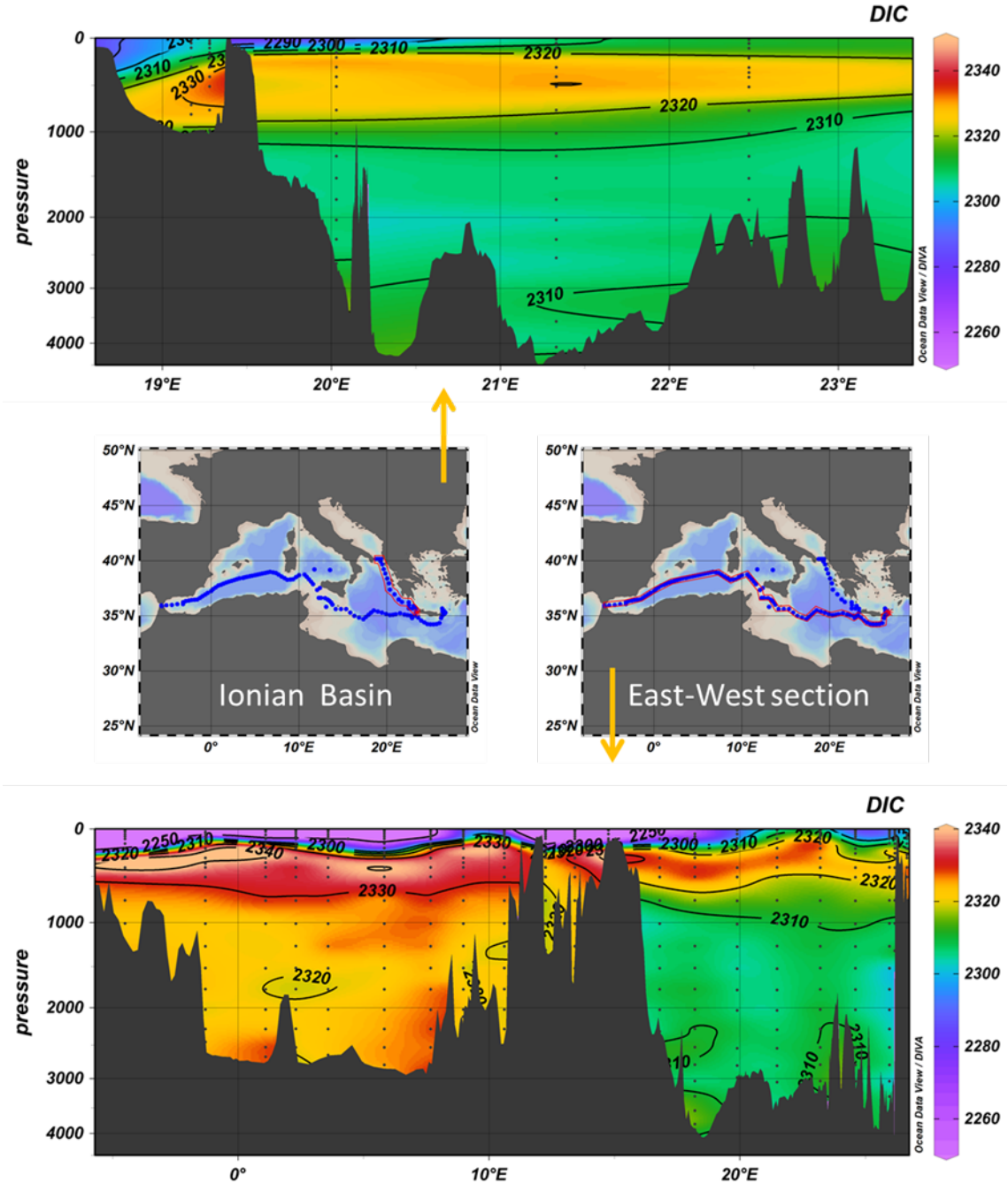

Fig. 5.5.6 DIC distribution in MSM72 cruise.

After blanking with the sampled seawater without dye, 50 µl of the dye solution were added to each sample using an adjustable repeater pipette (Eppendorf Multipette plus). Sample absorbance is measured at three fixed different wavelengths (λ_1 = 434 nm, λ_2 = 578 nm and λ_3 =730 nm) corresponding with the acidic and basic forms of the indicator corrected for baseline absorbance at λ_3. In addition, the sample absorbance was also measured at the isosbestic point (λ =487.6 nm). The pH value on the total hydrogen ion concentration scale at 25°C is calculated using the following formula defined by Clayton and Byrne (1993):

Fig. 5.5.7 Spectrophotometer, incubator and cells for pH measurements at Trokenlabor in the R/V Maria S. Merian.

$$pH_T = \frac{1245.69}{T} + 3.8275 + (2.11 \cdot 10^{-3})(35 - S) + \log\left(\frac{R - 0.0069}{2.222 - R\ 0.133}\right)$$

Where **R** is the ratio of the measured absorbance ($R = \frac{\lambda_2 - \lambda_3}{\lambda_1 - \lambda_3}$), **T** is temperature in Kelvin scale and **S** is the salinity of the sample.

In 2007, Yao et al. 2007 found some impurities in the m-CP that absorb at 434 nm, therefore, in higher values of pH. Recent studies suggest that those impurities should be removed from the m-cresol purple (unpur mPC) via high performance liquid chromatography (HPLC) (Liu et al., 2011). Liu and co-authors rewrote the pH_T definition as follow for the purified m-cresol purple (pur mCP):

$$pH_T = -\log(K_2^T e_2) + \log\left(\frac{R - e_1}{1 - R\,\frac{e_3}{e_2}}\right)$$

During MSM72, 75 stations were measured using the unpur mCP, and, from them, 9 stations were also measured with pur mCP.

As the injection of the indicator into the seawater perturbs the sample pH slightly, the absorbance ratios measured in the seawater samples (R_m) should be corrected to the R values that would have been observed in an unperturbed analysis (R_{real}). In order to do this, we obtain the correction in the absorbance ratio of every sample as a function of the absorbance ratio measured (R_m). This linear function was calculated from second additions of the indicator over samples with a wide range of pH (Figure 5.5.8 and 5.5.9):

Unpur mCP: $R_{real} = R_m - [(-0.0062 \pm 0.0016) * R_m + (0.0065 \pm 0.0028)]$ $R^2 = 0.1678$ n=73

Pur mCP: $R_{real} = R_m - [(-0.0062 \pm 0.0018) * R_m + (0.0098 \pm 0.0031)]$ $R^2 = 0.1757$ n=58

This function also corrects for deviations in the linear relationship between absorbance and the indicator concentration; i.e., deviations from the Beer Law in the spectrophotometer.

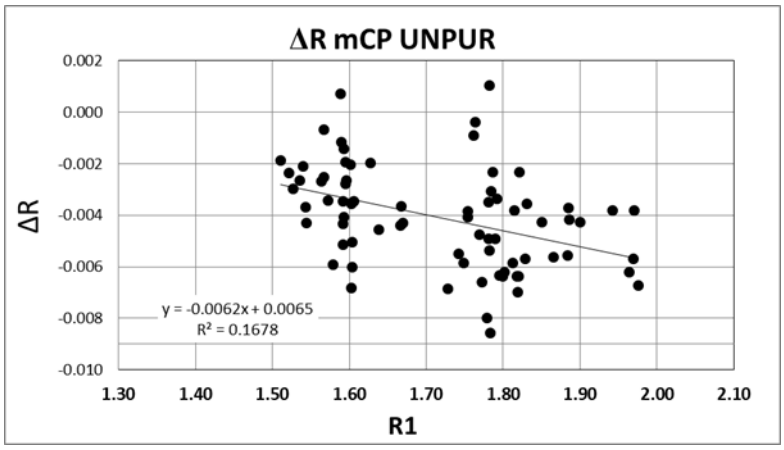

Fig. 5.5.8 Perturbation of sample pH induced by addition of unpur mCP, expressed as ΔR (R_2–R_1) as a function of R1.

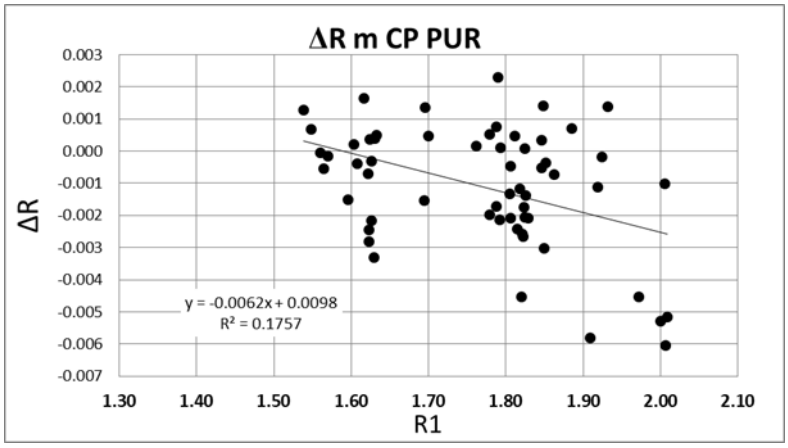

Fig. 5.5.9 Perturbation of sample pH induced by addition of pur mCP, expressed as ΔR (R_2–R_1) as a function of R1.

Accuracy

In order to check the accuracy of the pH measurements, samples of TRIS buffer certified seawater (distributed by A.G. Dickson from the Scripps Institution of Oceanography) were analysed during the cruise MSM72 at three different temperatures, in order to have representative pH values covered by the cruise in the Eastern and Western basins (Table 5.5.4).

Table 5.5.4 Mean temperature and pH, together with the standard deviation (STD) and number of samples of TRIS buffer.

Tª (°C)	pH	STD	n	Theoretic TRIS pH	Difference
25	8.0981	0.0008	4	8.0935	0.0046
27	8.0366	0.0014	3	8.0314	0.0051
29.7	7.9566	0.0024	4	7.9485	0.0090

The results show that our pH measurements are accurate as differ less than 0.005 pH units from the theoretical TRIS pH value at 25ºC.

Precision

Five samples from the same Niskin bottle were taken to perform a typical reproducibility analysis at Western basin (St 52 at bottom depth and St 56 at 100m) and Eastern basin (St 100 at bottom depth and St 102 at 100m). Table 5.5.5 shows the mean pH together with the standard

deviation and the number of samples collected. This repeatability exercise demonstrated that our precision is less than 0.001 pH units independently of the pH.

Table 5.5.5 Characteristics of the seawater and mean, standard deviation (STD) and number of cells collected from each Niskin at the different stations for the pH analysis.

St	Salinity	Depth (m)	pH	STD	n
52	38.727	3402.37	7.9590	0.0003	6
56	38.605	103.56	7.9737	0.0005	5
100	38.491	2764.03	7.8975	0.0004	4
102	38.045	104.75	7.9352	0.0008	4

In addition, from St 44 until the end of the cruise, when time and cells were available, double pH measurements at bottom and 100m were performed, with a total of 44 double samples. In table 5.5.6 a summary of those double samples is shown, confirming the good precision of our pH measurements.

Table 5.5.6 Ranges of depth and pH where double samples were taken, together with the Mean Absolute difference ($|pH_1-pH_2|$) and standard deviation of those differences. N is the number of double samples measured.

Depth range (m)	pH range	Mean Absolute difference	STD	n
70-150	7.8561-7.9837	0.0007	0.0004	22
400-3800	7.8816-7.9616	0.0007	0.0006	22

Results

The pH results obtained during the cruise MSM72 are shown in figure 5.5.10. The upper panel show the pH distribution along the Ionian Basin, while the lower panel show it along the longitudinal Eastern – Western basins, including the Cretan Waters.

5.5.3 Total alkalinity (TA)

TA along the MSM72 cruise was analysed following a double end point potentiometric technique by Pérez and Fraga (1987) further improved in Pérez et al. (2000). This technique is faster than the whole curve titration, with comparable results (Mintrop et al., 2000).

Sampling

Seawater samples for TA were collected after pH samples, in 600 ml borosilicate bottles and stored in the laboratory until analysis, no later than 2 days. Bottles were filled, overflowed and immediately sealed. Table 5.5.10 shows the selected stations for the TA samples.

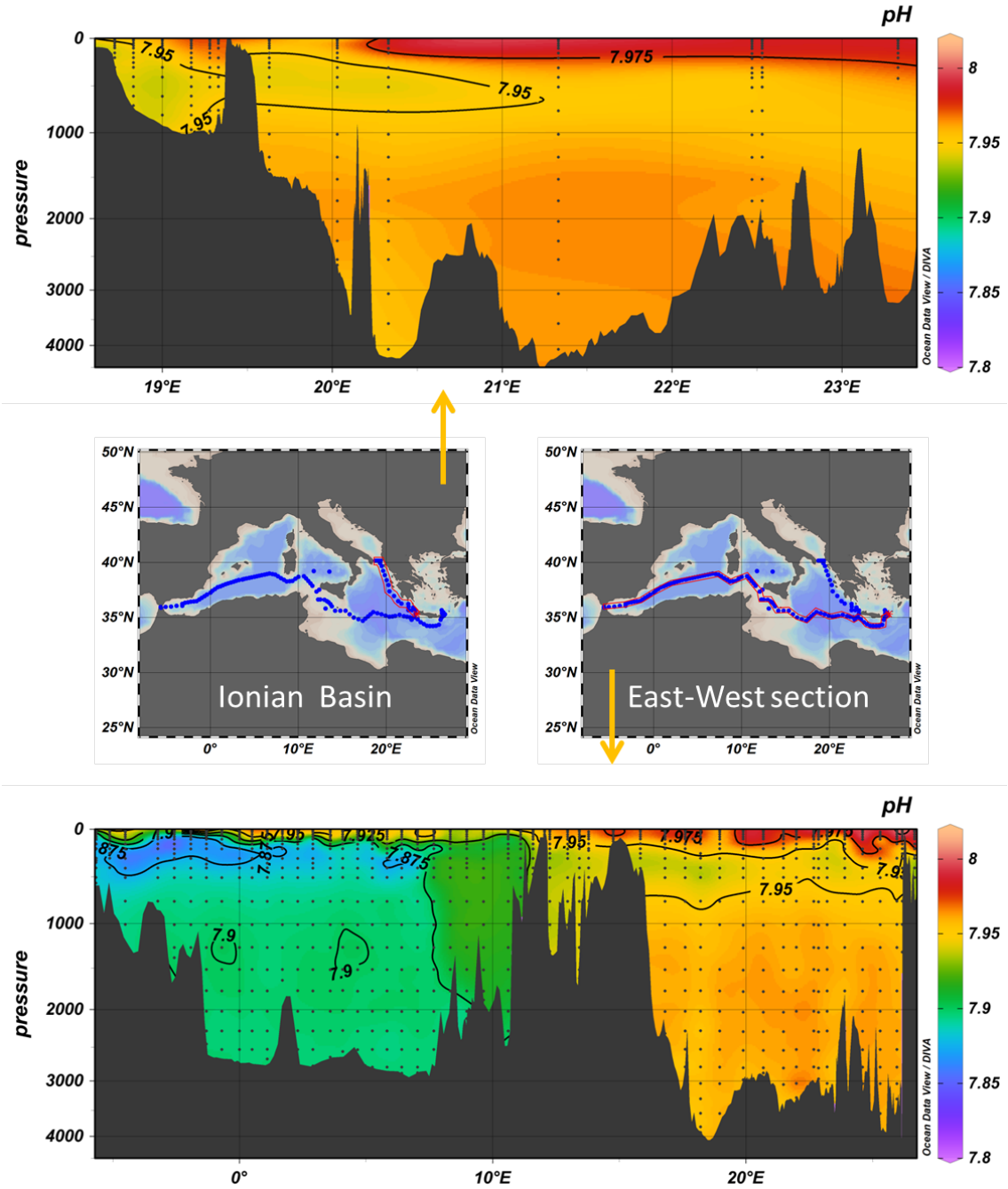

Fig. 5.5.10 pH distribution in MSM72 cruise.

Analytical method

TA was measured using an automatic potentiometric titrator "Titrando 904 Metrohm", with a Metrohm Aquatrode Plus combination glass electrode and a Pt-1000 probe to check the temperature. The system is coupled with a 5 mL burette or exchangeable unit. Potentiometric titrations were carried out with hydrochloric acid ([HCl] = 0.1 N) to a final pH of 4.40 (Pérez and Fraga, 1987). The electrodes were standardised using an ftatalate buffer of pH 4.41 made in CO_2 free seawater (Pérez et al., 2000). Concentrations are given in µmol kg^{-1}.The 0.1 N hydrochloric acid is prepared mixing 0.5 mol (18.231 g) of commercially HCl supplied by Riedel-deHaën (Fixanal 38285) with distilled water into a graduated 5L flask at controlled temperature conditions. The HCl normality is exactly refereed to 20°C. The variation of salinity after the titration is lower than 0.1 units, which is taken into account in the final TA calculation.

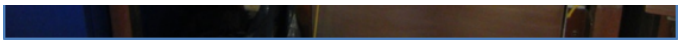

Fig. 5.5.11 Titrando 904 and stirrer 801 (Metrohm) where the TA samples are titrated.

Faced problems

Normally, the 0.1 N HCl is prepared following the aforementioned methodology. However, the available reagent aboard the ship was Titrisol® Hydrochloric acid for 1000 ml ([HCl] = 1N) supplied by Sigma-Aldrich. As we only had two 5L flasks, we prepared 5L of [HCl] = 0.2N, and then, diluted it until approximately 0.1N with two graduated flasks (500 and 1L) borrowed from our colleagues in the ship. Since the HCl concentration has to be precise, around 500ml of each three batches of HCl prepared along the cruise were stored to be titrated at the INOCEN lab at IEO-A Coruña.

Certified Reference Material

In order to control the accuracy of TA measurements, Certified Reference Material (CRM) of CO_2 analyses were performed in every TA analysis session at the beginning of each session. Those CRM were batch #158 (TA = 2226.55 ± 0.80 µmol/kg) and batch #170 (TA = 2198.77 ± 0.87 µmol/kg), provided by Prof. Andrew Dickson. Figures 5.5.12 and 5.5.13 show the obtained TA values for each CRM, where the grey squares are the measured TA values and the circles represent the mean value with the corresponding error bar per analysis session.

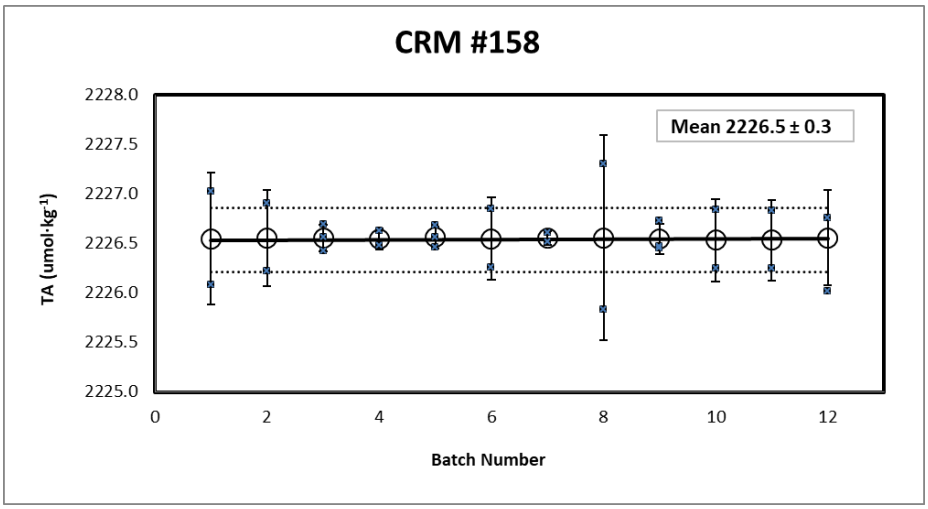

Fig. 5.5.12 Alkalinity (µmol kg-1) measurements on the CRM batch #158 during the cruise in function of the batch number (batches 1-12).

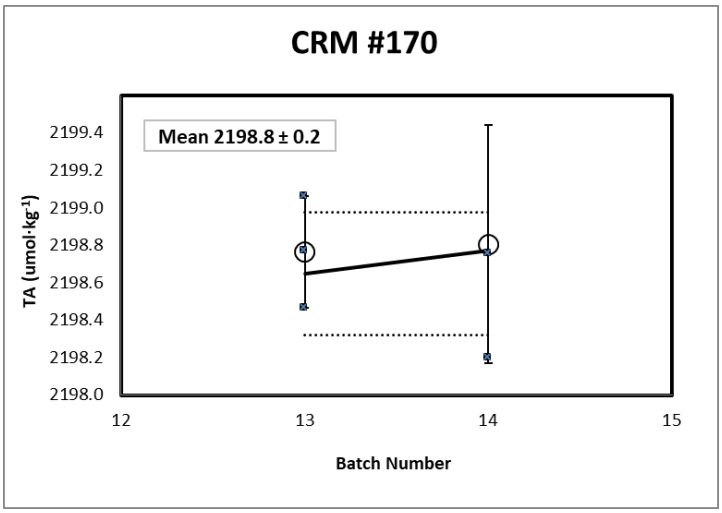

Fig. 5.5.13 Alkalinity (µmol kg-1) measurements on the CRM batch #170 during the cruise in function of the batch number (batches 13-14)

Substandard

In addition, an extra calibration was conducted during the cruise MSMS72 by analysing samples of substandard seawater at the beginning, during and at the end of each batch of samples. The seawater substandard SUB1 consisted of 700m seawater coinciding with the minimum salinity at St2 (38.91), while SUB2 is deep seawater from 2297.62m and salinity 38.52 (St 84), both stored in dark into a large container (30L) at least one day before its use. The repeated analysis of this water is the reference used to monitor the drift of the TA determinations with time during whole cruise (Figure 5.5.14 and 5.5.15)

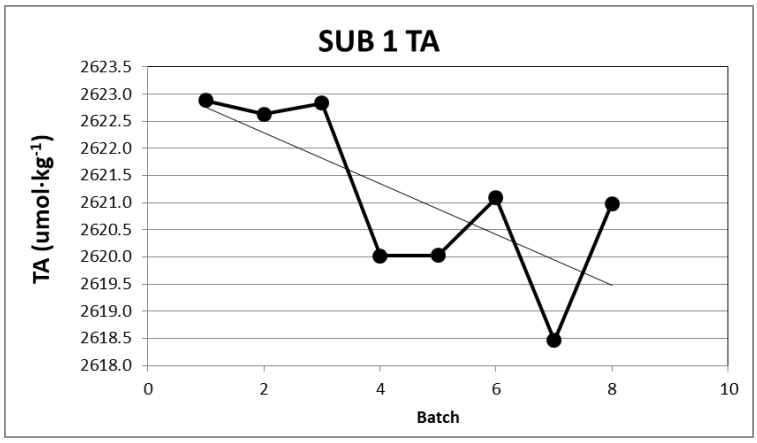

Fig. 5.5.14 TA measurements for the substandard seawater represented against batch of analysis (batches 1-8)

In Table 5.5.7 a summary of both CRM and substandard quality control for TA analysis is given. ΔpH is the pH correction applied to relate the TA determinations on the CRM to the corresponding nominal value for CRM batches #158 and #170. The mean value of the TA measurements on the CRM samples is shown (Fitted TA ± standard deviation). The mean value of the TA measurements on the substandard samples is also shown (Mean SUB TA ± standard deviation). Av. Dif. and number of duplicates is the average of the difference in the duplicate's analyses.

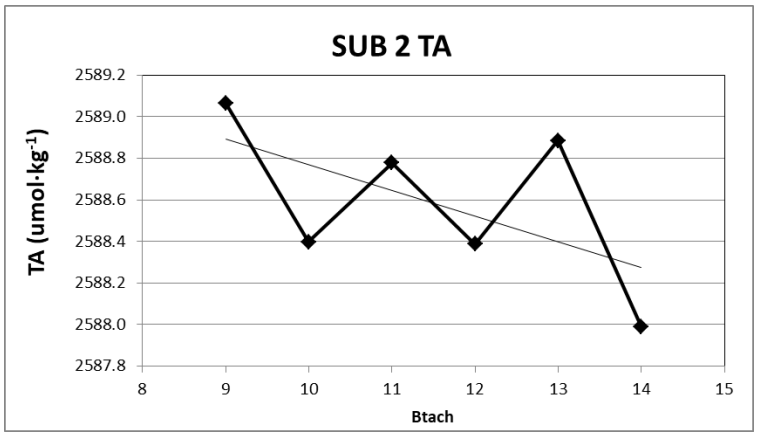

Fig. 5.5.15 TA measurements for the substandard seawater represented against batch of analysis (batches 9-14)

Table 5.5.7 Evaluation of the drift in the TA measurements by analysis of a CRM and substandards. All TA values in µmol/kg.

Batch	Day 2018	ST	ΔpH	Fitted TA	Mean SUB TA	Av. Dif
1	4 March	1, 2, 4, 8	0.01215	2226.55±0.67	2622.88±0.30	0.79 (47)
2	5 March	9, 11, 13	0.01315	2226.55±0.48	2622.63±0.42	0.68 (47)
3	7 March	17, 20	0.0247	2226.55±0.13	2622.84±0.34	0.38 (28)
4	9 March	22, 23, 26	0.00495	2226.55±0.10	2620.02±0.91	0.56 (54)
5	13 March	30, 32, 34, , 38, 40, 42, 43	0.0091	2226.56±0.11	2620.03±0.64	0.49 (82)
6	16 March	44, 47, 51, 53	0.032	2226.55±0.42	2621.09±0.36	0.61 (85)
7	17 March	55, 57, 59, 61, 63	0.0348	2226.55±0.07	2618.46	0.55 (76)
8	21 March	66, 68, 70, 72, 73, 75	0.0423	2226.56±1.04	2620.98±0.58	0.70 (77)
9	24 March	77, 79, 81, 83, 85, 87, 89	0.0421	2226.54±0.15	2589.07±0.47	0.57 (80)
10	26 March	91, 93, 95, 97	0.0225	2226.53±0.42	2588.40±0.35	0.68 (72)
11	27 March	100, 101, 102, 105	0.0125	2226.53±0.41	2588.78±0.19	0.69 (43)
12	29 March	109, 111, 113, 115	0.0108	2226.56±0.48	2588.39±0.34	0.60 (67)
13	31March	119, 121, 125, 128	0.0115	2198.76±0.30	2588.88±0.27	0.55 (62)
14	1 April	130, 132, 134, 136	0.009	2198.81±0.64	2587.99±0.39	0.61 (38)

Precision

Five samples from the same Niskin bottle were taken to perform a typical reproducibility analysis at Western Basin (St 52 at bottom depth and St 56 at 100m) and Eastern Basin (St 100 at bottom depth and St 102 at 100m). Table 5.5.8 shows the mean TA together with the standard deviation and the number of samples collected.

Table 5.5.8 Mean, standard deviation (STD) and number of samples collected from each Niskin at the different stations for the TA analysis .

St	Salinity	Depth (m)	TA (µmol/kg)	STD	n
52	38.727	3402.42	2610.9	0.65	5
56	38.605	103.72	2581.0	0.66	5
100	38.491	2764.34	2585.65	0.27	6
102	37.857	104.36	2540.30	0.45	5

In addition, duplicate analysis for a total of 730 samples was performed, one immediately after the other, in all measured stations, with a mean standard deviation of those TA duplicates of 0.6 μmol Kg^{-1}. So, we consider the error of our TA measurements lower that 1 μmol Kg^{-1}.

Results

The TA results obtained during the cruise MSM72 are shown in figure 5.5.16. The upper panel show the TA distribution along the Ionian Basin, while the lower panel show it along the longitudinal Eastern – Western basins, including the Cretan Waters.

5.5.4 Carbonate ion concentration (CO_3^{2-})

The carbonate ion concentration (CO_3^{2-}) was determined spectrophotometrically following the recent method first proposed by Patsavas et al. (2015), after the works of Byrne and Yao (2008) and Easley et al. (2013). The spectrophotometer used to analyse CO_3^{2-} samples is the same used for pH measurements (see figure 5.5.1).

Sampling

CO_3^{2-} samples were taken after TA. Samples were collected in cylindrical optical quartz 10cm pathlength cuvettes, which were filled, overflowed and immediately sealed. After sampling, the cells are immediately stabilised at 25°C in the same incubator as for the pH cells. The sampling scheme of CO_3^{2-} is showed in Table 5.5.10.

Analytical method

The concentration of CO_3^{2-} in seawater was measured using the method proposed by Patsavas et al. (2015). A solution of 0.022 M of the titrant $Pb(ClO_4)_2$ (Fisher Scientific, 99.99% purity dissolved in distilled water) is added to the seawater sample, the complex PbCO3 formed afterwards is detected spectrophotometrically in the UV spectra. All the absorbance measurements were obtained in the thermostatic (25±0.2°C) cell compartment of the UV-Vis 2600 SHIMADZU double beam spectrophotometer. The temperature was controlled with a JULABO F12 ED (12L) cryostatic bath.

After blanking with the sampled seawater without the lead solution, 20 μl of the dye solution was added to each sample using an adjustable repeater pipette (Eppendorf Multipette plus). The absorbance was measured at three different three wave lengths: λ_1 (234 nm) is the UV absorbance wavelength at the isobestic point of $PbCO_3$, λ_2 (250 nm) is the mean value of the wavelength presenting high absorbance variation and λ_3 (350 nm) is a non-absorbing wavelength to monitor $PbCO_3$.

Total carbonate ion concentration ($[CO_3^{2-}]$) is given by:

$$-\log[CO_3^{2-}]_T = \log_{CO3}\beta_1 + \log\left(\frac{R - e_1}{e_2 - R \cdot e_3}\right)$$

where R is the ratio of the absorbances (A) ($R = \left(\frac{\lambda_2 - \lambda_3}{\lambda_1 - \lambda_3}\right)$), $_{CO3}\beta_1$ is the $PbCO_3$ formation constant, and e_i are the molar absorptivity ratios dependent on salinity. The fitting parameters are taken from Patsavas et al. (2015).

Precision

Five samples from the same Niskin bottle were taken to perform a typical reproducibility analysis at Western basin (St 52 at bottom depth and St 56 at 100m) and Eastern basin (St 100 at bottom depth and St 105 at 100m). Table 5.5.9 shows the mean CO_3^{2-} together with the standard deviation and the number of samples collected.

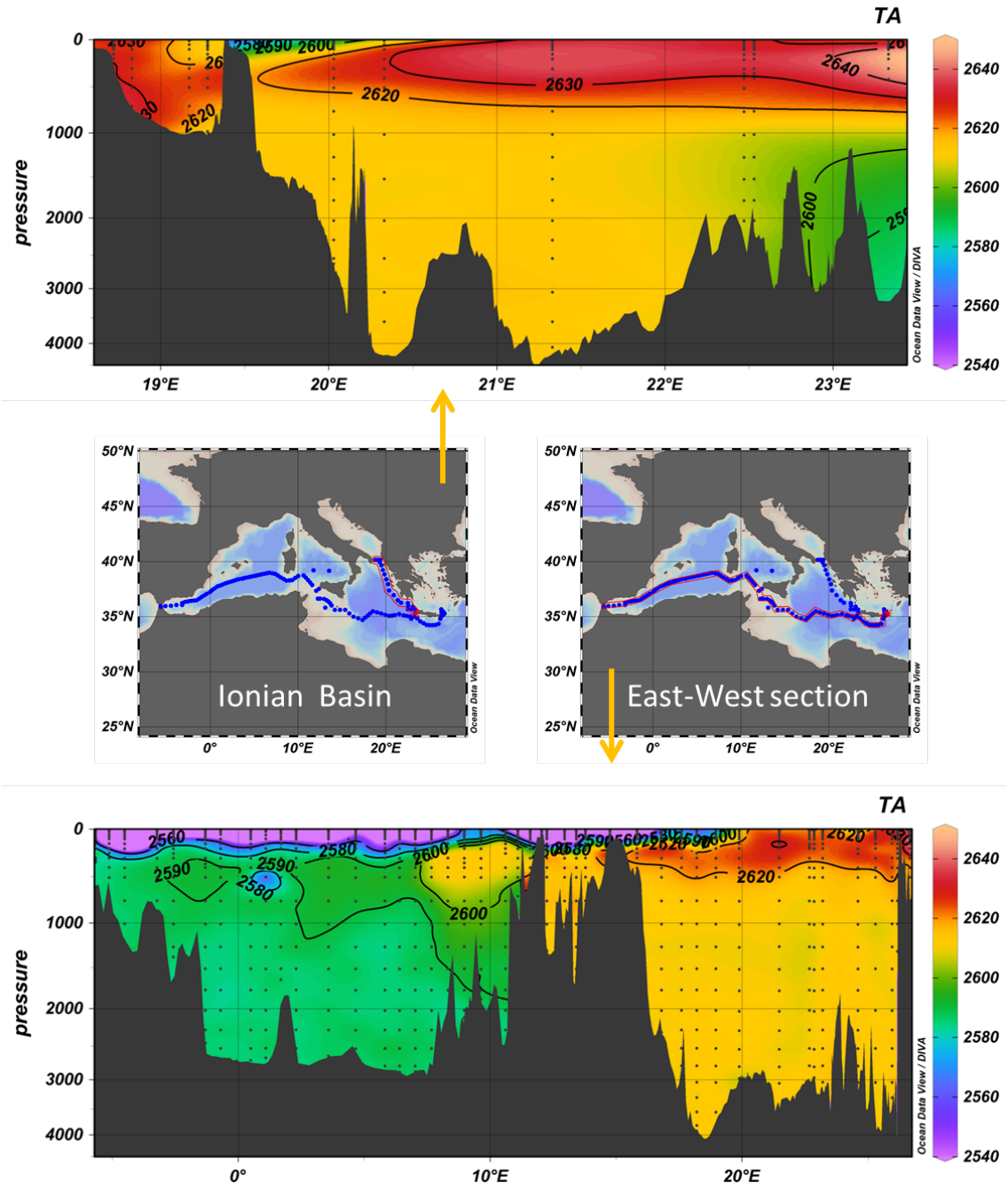

Fig. 5.5.16 TA distribution in MSM72 cruise.

Table 5.5.9 Mean, standard deviation (STD) and number of cells collected from each Niskin at the different stations for the CO_3^{2-} repeatability analysis.

St	Salinity	Depth (m)	CO_3^{2-} (µmol/kg)	STD	n
52	38.727	3402.42	244.8	1.13	5
56	38.605	103.72	256.9	0.93	5
100	38.491	2764.34	215.3	1.13	5
105	37.857	104.36	234.8	0.41	5

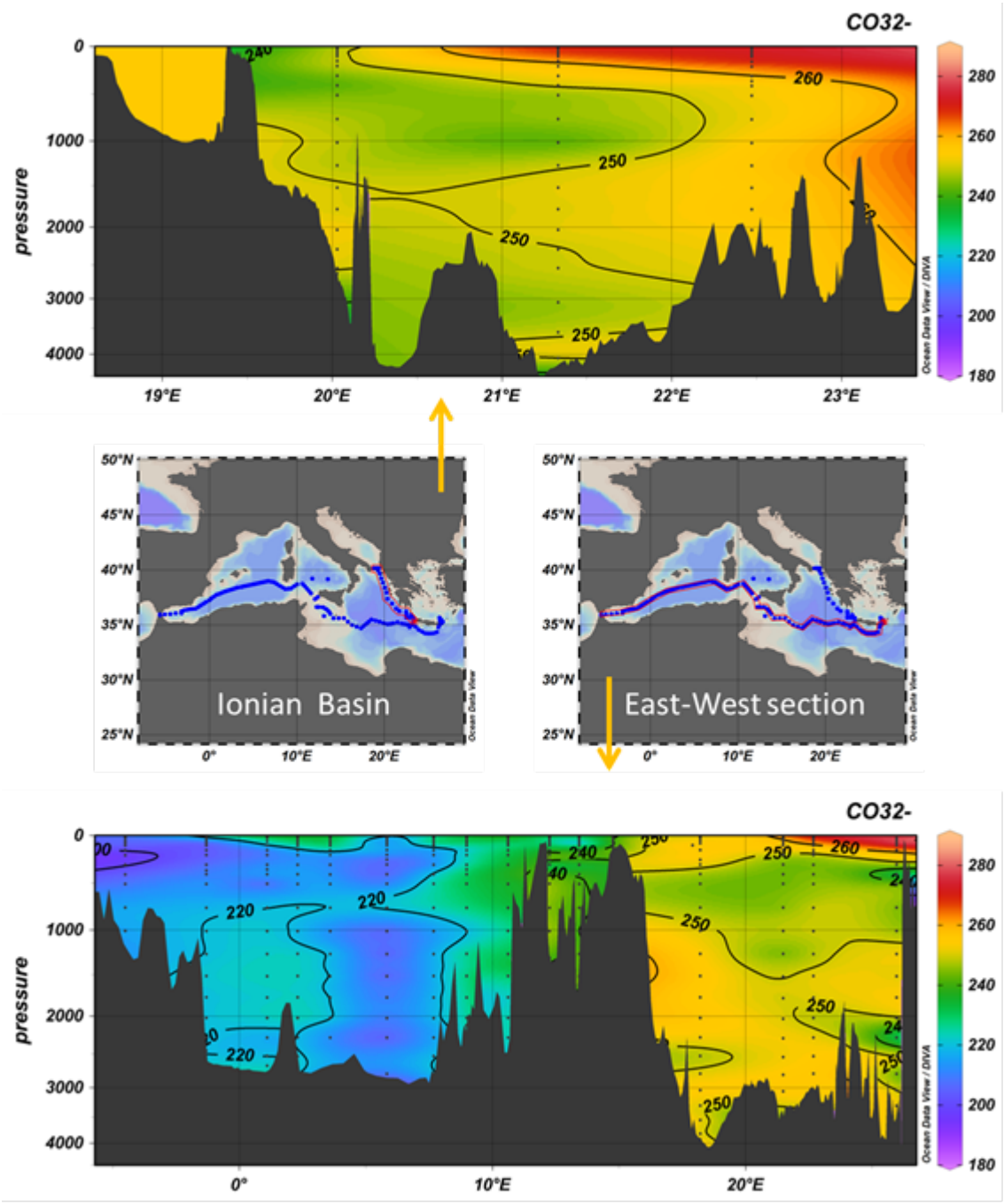
CO32-
pressure
0
1000
2000
3000
4000
19°E
20°E
21°E
22°E
23°E
240
250
260
280
180
200
220
Ocean Data View / DIVA
50°N
45°N
40°N
35°N
30°N
25°N
0°
10°E
20°E
Ionian Basin
East-West section
Ocean Data View

Fig. 5.5.17 CO_3^{2-} distribution in MSM72 cruise.

Results

The CO_3^{2-} results obtained during the cruise MSM72 are shown in figure 5.5.17. The upper panel show the CO_3^{2-} distribution along the Ionian Basin, while the lower panel show it along the longitudinal Eastern – Western basins, including the Cretan Waters.

Sampling scheme

The table 5.5.10 shows the number of stations, samples, and the number of Niskin bottles at different depths, where CO_2 variables were measured. Note that in the pCO_2 column, "1" means that one sample of pH and TA were taken until station 73, and from station 75 until the end of the cruise one surface sample of surface DIC, pH and TA were taken.

Table 5.5.10 Number of samples taken at each station for each individual variable.

ST	Depth	DIC	pH	TA	CO_3^{2-}	pCO_2
1	313	5	5	5		
2	2368	19	19	19	19	
4	741	14	14	14		
8	1150	14	14	14		
9	3700	23	46	23	23	
11	3450		21	15		
13	3000	20	20	20		
15	3000		19			
17	3100	21	21	21		1
20	400		9	9		
22	2928		20	20		
23	4603	19	22	22	22	1
26	3200		22	22		1
30	4100	19	22	22	22	
32	4200		22	14		
34	2500	18	19	19	19	1
36	1400		15			
38	1000	11	13	13		
39	950		10			
40	1000	10	15	10		
41	950		11			
42	800		14	9		
43	500	8	11	11		
44	3300		24	22	24	
46	3200		21			
47	3400	17	48	21	21	1
49	2800		22			
51	3000	16	22	20		1
52	3200	5	10	5	5	1
53	3800		24	22		
55	4000	20	24	22	22	1
56	3600	5	10	5	5	

57	2800		44	20		
59	2200	14	19	17		
61	500		12	10		
63	500	4	14	6	6	
66	1100		14	14		1
68	1800	16	32	16	16	
70	1000		13	13		
72	1400	14	14	14	14	1
73	100		5	5		1
75	3500		21	21		1
77	3200	21	42	21	21	1
79	500		10	10		
81	800		11	11		
83	2600	19	19	19	19	1
85	1800		16	16		
87	2200	19	19	19	19	1
89	2100		24	22		
91	2900	20	40	20	20	1
93	2800		20	20		
95	2900		20	20		
97	2800	21	21	21	21	1
99	2800		23			
100	2700	5	10	5	5	
101	2600		19	19		
102	2500	5	10	5		
103	2500		19			
105	2600	18	30	18	23	1
107	2600		22			
109	2500	19	21	19	19	
111	1500		15	15		
113	2600	19	37	19	19	1
115	2600		19	19		
117	2600		19			
119	2600		19	19		
121	2500	18	36	16	18	1
123	1350		12			
125	1340		24	12		1
128	1300		12	12		
130	1300	13	26	13	13	1
132	600		9	9		
134	350		9	9		
136	500		10	10		

First quality control

A first visual inspection of the vertical distribution of DIC (Table 5.5.11), pH (Table 5.5.12), TA (Table 5.5.13) and CO_3^{2-} (Table 5.5.14) were done, helping to identify questionable data along the MSM72 cruise. The questionable data were flagged as 3, good data as 2 and not measured as 9.

Table 5.5.11 DIC questionable data.

Station	Cast	Niskin
2	1	19
2	1	21
2	2	2
2	2	4
2	2	6
2	2	8
2	2	10
2	2	12
2	2	14
2	3	12
4	1	8
4	1	10
9	1	7
72	1	8
113	1	7
113	1	8

Table 5.5.12 pH questionable data

Station	Cast	Niskin
1	1	5
2	1	17
9	2	11
9	2	13
9	2	15
11	2	17
13	1	10
22	1	14
32	1	8
32	1	16
34	1	17
34	2	10
41	1	1
46	1	5
46	1	13
70	1	4
91	1	10
113	2	8
115	1	1
117	1	16
119	1	11
119	1	12
132	1	1

Table 5.5.13 TA questionable data

Station	Cast	Niskin
4	1	8
4	1	10
4	1	14
11	2	13
23	1	17
42	1	19
43	1	17
51	1	1
66	1	10
66	1	11
68	1	13
68	1	14
68	1	15
68	1	17
75	2	21
89	1	14
113	1	1
113	1	9
130	2	11
132	1	7
134	1	9

Table 5.5.14 CO_3^2 questionable data

Station	Cast	Niskin
2	1	6
2	1	13
2	2	8
9	1	12
9	2	8
30	1	1
30	1	11
30	1	21
44	1	6
47	1	1
55	1	4
55	1	11
63	1	3
63	1	6
68	1	1
68	1	7
68	1	17
72	1	1
72	1	6
72	1	9
72	1	10
72	1	12
72	1	13
77	1	1
77	1	2
77	1	5
77	1	7
77	1	8
77	1	9
77	1	10
77	1	11
77	1	12
77	1	13
77	1	14
77	2	1
77	2	5
87	1	6
87	1	13
87	1	15
91	1	3
91	1	4
91	1	6
91	1	13
97	1	1
97	1	7
97	1	8
97	1	9
97	1	11
97	1	12
97	1	13
97	2	1
97	2	5
97	2	6
97	2	9
97	2	11
97	2	12
105	1	3
105	1	5
105	1	6
105	1	8
109	1	17
113	1	1
113	1	8
113	1	11
113	1	15
113	2	3
130	2	1

5.6. Measurements of CFC-12 and SF_6 (Toste Tanhua , Nico Lange, Fabian Wolf, Lennart Gerke)

Analysis System Setup:

During the cruise, one GAS CHROMATOGRAPH / PURGE-AND-TRAP (GC/PT) system (PT3, figure 5.6.1) was used for the measurements of the transient tracers CFC-12 and SF_6. The system is modified versions of the set-up normally used for the analysis of CFCs (Bullister and Weiss, 1988).

The traps consisted of 100 cm 1/16" tubing packed with 70cm Heysep D kept at temperatures between -70 and -75°C during trapping. The traps were desorbed by heating to 120°C and passed onto the pre-columnn. The pre-column consisted of 20 cm Porasil C followed by 20 cm Molsieve 5A in a 1/8" stainless steel column. The main column was a 1/8" packed column consisting of 180 cm Carbograph 1AC (60-80 mesh) and a 50 cm Molsieve 5A post-column. Both columns were kept isothermal at 60°C. Detection was performed on an Electron Capture Detector (ECD).

All samples were collected in 250 mL ground glass syringes, of which an aliquot about 200 mL was injected to the purge-and-trap system, normally within 5 hours from sampling.

Standardization was performed by injecting small volumes of gaseous standard containing CFC-12 and SF_6. This working standard was prepared by the company Dueste-Steiniger (DS1,). The CFC-12 and SF_6 concentrations in the working-standard has been calibrated vs. a reference standard obtained from R.F Weiss group at SIO, and the CFC-12 data are reported on the SIO98 scale. Calibration curves were measured roughly once a week in order to characterize the non-linearity of the system, depending on workload and system performance. Point calibrations were always performed between stations to determine the short-term drift in the detector. Replicate measurements were taken except for near coastal stations due to high workload. To assess the reproducibility of the set-up, 50 replicates samples were run, and resulted in a reproducibility of 1.0 % or 0.01 pmol kg^{-1} for CFC-12 and 2.3% or 0.03 fmol kg^{-1} for SF_6. In total we successfully measured 1084 samples on 68 stations for transient tracers.

In addition to the on-board analysis, on three stations (#52, #84, and #106) 1500 ml glass ampoules were flame sealed for later analysis in the lab in Kiel for the detection of novel halogenated tracers such as HFC134a and HCFC22. The measurements will be performed on the "Medusa" purge-and-trap GCMS.

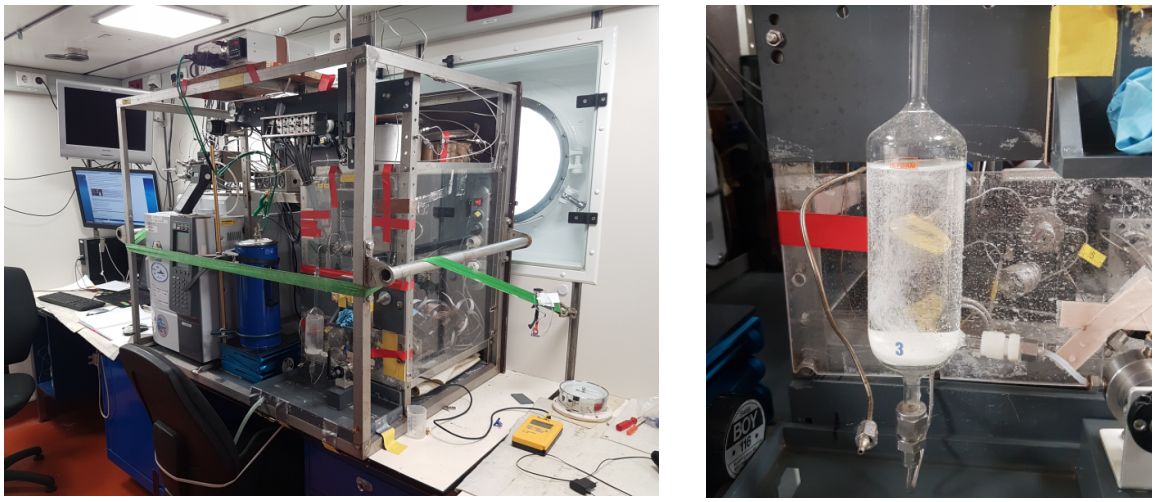

Fig. 5.6.1 Analytical setup during MSM72; left panel - the purge and trap system (PT3), left panel – the purge chamber during purging of a water sample.

Preliminary results:

The Mediterranean Sea is well ventilated and we find significant concentrations of SF_6 and CFC-12 on all stations and on all depths (figure 5.6.2). For most stations we find a minimum of tracer concentration around 1000 m depth and then an increase towards the depth again, this is an unusual profile shape for transient tracers in the world ocean, and is particularly pronounced in the Western Basin that has seen intense deep water formation for the last decade.

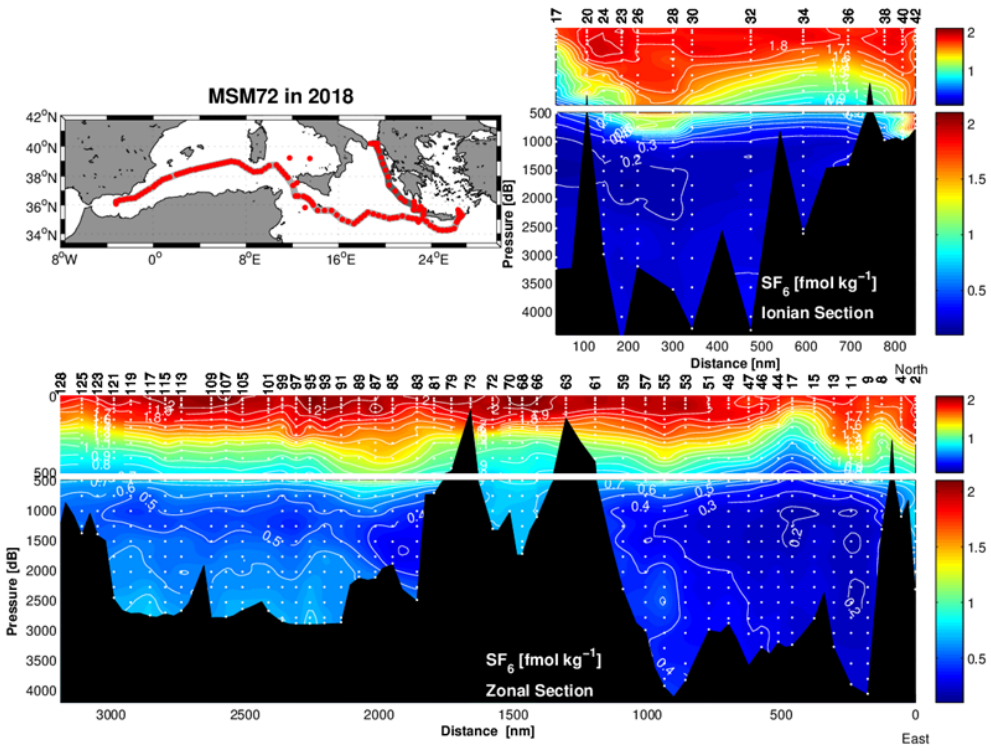

Fig. 5.6.2 Section of SF_6 through the Mediterranean Sea, preliminary data.

5.7. DOC and CDOM Sample Collection

(Giancarlo Bachi, Chiara Santinelli)

Marine dissolved organic matter (DOM) is constituted by carbon (DOC, ~93%), nitrogen (DON, ~7%) and phosphorus (DOP, ~0.3%). DOM represents the largest ocean reservoir of reduced carbon (662·1015 g C) on the Earth, it therefore plays a major role in the global carbon cycle. Its role in the functioning of marine ecosystems is equally crucial in that DOM is released at all levels of the food web, as a byproduct of many trophic interactions and/or metabolic processes and is the main resource for heterotrophic prokaryotes (Carlson and Hansell, 2015). Although most DOM is produced in-situ, external sources (atmosphere, rivers, sediments) affect its concentration and distribution (Santinelli et al., 2015, Santinelli, 2015). Physical processes, such as deep water formation, thermohaline circulation, vertical stratification and mesoscale activities are the main drivers of its distribution (Santinelli, 2015, Santinelli, 2010, Santinelli et al., 2013). A different functioning of the microbial loop was also observed in the western and eastern basin (Santinelli et al., 2012). The DOC data collected during the MSM72 cruise represents an unique opportunity to (i) investigate the long-term variation in DOC distribution in intermediate and deep waters on a basin scale; (ii) quantify the role of DOC in C export and sequestration in the Mediterranean Sea; (iv) estimate DOC mineralization rates; (v) asses the functioning of microbial loop in the different areas of the Mediterranean Sea.

Chromophoric DOM (CDOM) is the fraction of DOM that absorbs light over a broad range of ultraviolet (UV) and visible wavelengths, playing a key role in marine ecosystem. CDOM is the major factor controlling the attenuation of UV radiation in the ocean (Nelson & Siegel, 2013); its absorption in the coastal areas can reduce the visible light available for photosynthesis, with a reduction of primary production. Though terrestrial inputs (rivers and atmosphere) represent an important source of CDOM, it is also produced in-situ by biological activity and it is mainly removed by photochemical degradation and microbial consumption. Deep ocean circulation drives its distribution (Nelson & Siegel, 2013). The study of the absorption and fluorescence properties of CDOM, in particular the analysis of the excitation-emission matrixes (EEMs) with the parallel factorial analysis (PARAFAC) can give some qualitative information, such as: (i) the occurrence of different kind of chromophores (protein-like, humic-like and PAH-like), (ii) the changes in CDOM due to photodegradation and/or microbial transformation, (iii) the main sources of CDOM, (iv) an indirect estimation of its molecular weight and aromaticity degree (Stedmon and Nelson, 2015, Retelletti et al., 2015, Gonelli et al., 2016, Margolin et al., 2018). The CDOM data collected during the MSM72 cruise in all the stations and along the whole water column will represent an unique opportunity to: (i) Compare CDOM optical properties in the different water masses of the Mediterranean Sea with those collected in the Geotraces cruise (Spring-summer 2013) and to relate them to the different trophic conditions of the basin; (ii) Study the relationship between DOC and CDOM in the surface, intermediate and deep waters

Sample collection

Seawater samples were collected from the CTD-Rosette systme into 250 ml Polycarbonate Nalgene bottles. Samples were filtered through a 0.2 µm Nylon filter under high-purity air pressure. For DOC analysis, filtered samples were collected in 60 ml Nalgene bottles, acidified

and stored at 4°C and in the dark. For CDOM analysis, filtered samples were collected in 100 ml glass dark bottles and stored at 4°C and in the dark.

Method and instruments used

5.7.1 DOC

DOC measurements will be carried out with a Shimadzu Total Organic Carbon analyzer (TOC-Vcsn, S/N: H51204430133), by high temperature catalytic oxidation. Samples will be acidified with HCl 2N and sparged for 3 minutes with CO_2-free pure air, in order to remove inorganic carbon. One hundred and fifty µl of sample is injected in the furnace (680°C) after rinsing with the sample three times. From 3 to 5 replicate injections will be performed until the analytical precision is lower than 1% (± 1µM). A five-point calibration curve will be done by injecting standard solutions of potassium hydrogen phthalate in the expected concentration range of the samples. At the beginning and end of each analytical day the system blank will be measured using low carbon water (LCW) and the reliability of measurements will be controlled by comparison of data with a DOC reference (CRM) seawater sample kindly provided by Prof. D.A. Hansell of the University of Miami (http://yyy.rsmas.miami.edu/groups/biogeochem/CRM.html). DOC concentrations will be calculated by the equation:

$$DOC\ (\mu M) = \frac{(sample\ area - system\ blank\ area)}{slope\ of\ standard\ curve}$$

This procedure will guarantee the quality of the data and the possibility to compare them with those previously published and produced in other laboratories. For further analytical details refer to (Santinelli et al., 2015, Santinelli et al., 2013).

5.7.3 CDOM

Absorption measurements:

Absorbance spectra will be measured throughout the UV and visible spectral domains (230–700 nm) using a spectrophotometer UV-visible (Jasco Mod-7850, S/N: C02951782), with a 10 cm quartz cell. Milli-Q water is used as reference and its spectrum is subtracted from each sample. The absorbance (A) is converted into absorption coefficients (a) as follows:

$$a_{(\lambda)} = 2.303\ A(\lambda)/l$$

where A(λ) is the absorbance at wavelength λ and l is the pathway expressed in meters. Absorption coefficient at 280 nm (a_{280}) and 355 nm (a_{355}) are calculated in order to gain information on protein-like (a_{280}) and humic-like (a_{355}) substances. The spectral slope (S), is calculated in the range 275-295 nm, using the following fitting equation, where a_{λ_0} is the absorption coefficient at λ_0. For further analytical details refer to [14-16].

$$y = a_{\lambda_0}\, e^{-S\,(\lambda-\lambda_0)}$$

5.7.4 Fluorescence measurements

Fluorescence excitation-emission matrixes (EEMs) will be measured by using the Aqualog fluorometer (Horiba, S/N: 0119S-0412-AL), with a 10 × 10 mm^2 quartz cuvette. Excitation wavelength ranges between 250 and 450 nm at 5 nm increment, while emission spectra are measured between 212 and 619 nm at 3 nm increment. Each EEM is corrected for any inner-

filter effect and for instrument bias in excitation and emission. EEMs are subtracted by the blank EEM measured by using Milli-Q water. Rayleigh and Raman scatters are removed by interpolating the data using a monotone cubic interpolation (shape-preserving). Finally, the fluorescence intensity value is normalized by the integrated Raman band of Milli-Q water (λ_{ex} = 350 nm, λ_{em} = 371–428 nm), measured at the same day of the analysis. For further analytical details refer to Retelletti et al., 2015, Gonelli et al., 2016, Margolin et al., 2018.

Statistics

In total 650 samples were collected in 38 stations, the position of the stations is reported in the map below (Fig. 5.7.1). Samples were collected at the following standard depth: 10, 25, 50, 75, 100, 150, 200, 300, 400, 500, 750, 1000 and every 250 m until the bottom.

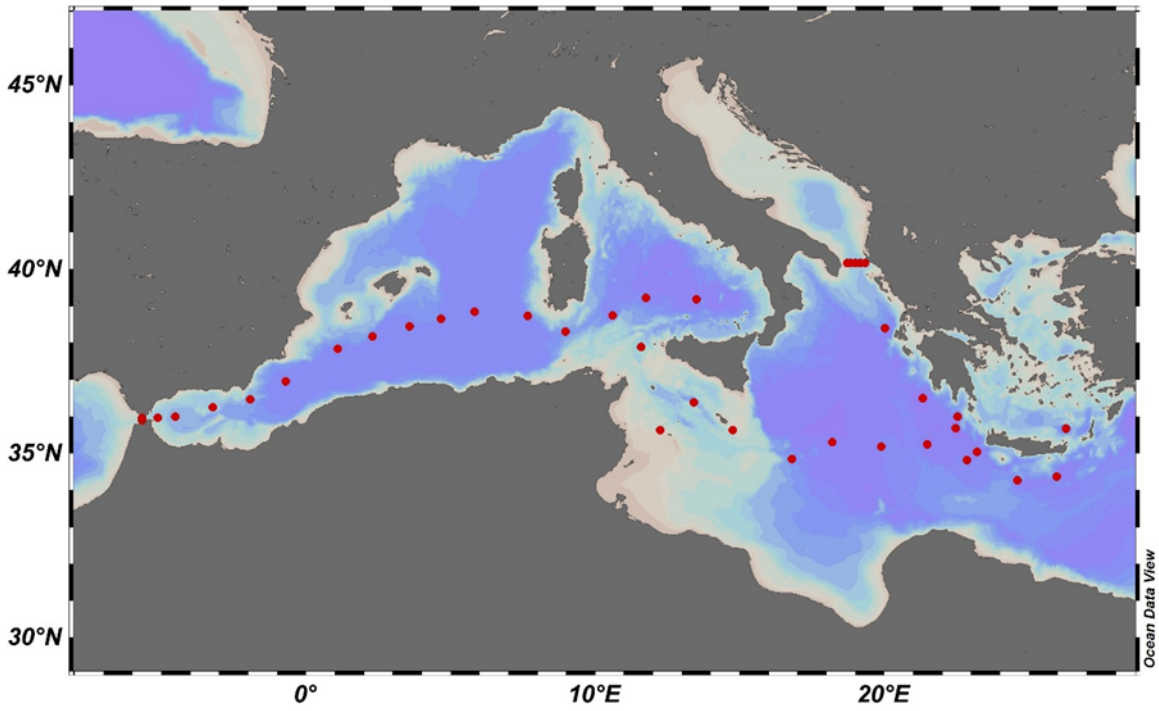

Fig. 5.7.1 Map of the station sampled by CNR-IBF

Data Quality

Data will be quality checked by visually analyzing the vertical profiles. The use of the certified international DOC reference material (CRM):

http://yyy.rsmas.miami.edu/groups/biogeochem/CRM.html
will ensured the quality of the data and their inter-calibration with data previously collected or produced in other laboratories.

5.8. Sampling for Measurements of Stable Carbon Isotopes on Dissolved Inorganic Carbon (DIC)

(Toste Tanhua)

Samples for the determination of stable carbon isotopes ($\delta^{13}C$) of Dissolved Inorganic Carbon (DIC) were taken on 11 stations (the "isotope stations", normally performed as a double cast) in the various basins along the cruise-track. In total 214 samples were taken in 100 ml dark glass bottles immediately poisoned with 100 µL saturated mercury chloride. The samples were measured off-line during fall of 2018 at the Centre for Isotope Research (CIO), Energy and Sustainability Research Institute Groningen (ESRIG), University of Groningen.

5.9. LISST – DEEP (serial number 4004*)*

(Spyros Chaikakis)

The LISST-Deep instrument obtains in-situ measurements of particle size distribution, optical transmission, and the optical volume scattering function (VSF) at depths down to 3,000 meters. It is manufactured by Sequoia Inc., and owned by the Hellenic Centre for Marine Research (HCMR) – Greece.
Using a red 670nm diode laser and a custom silicon detector, small-angle scattering from suspended particles is sensed at 32 specific log-spaced angle ranges. This primary measurement is post-processed to obtain sediment size distribution, volume concentration, optical transmission, and Volume Scattering function. The LISST-Deep s/n 4004 is categorized as a type B instrument, which means that the range of particles it measures ranges from 1.25 µm to 250 µm. The LISST-Deep must be powered externally at all times. This is typically achieved by connecting it to a rosette, getting power from the main CTD unit.

Parameters measured

- Particle size distribution from 1.25-250µm or 2.5-500µm
- Depth (3000 m max depth @ 0.8 m resolution)
- Optical transmission @ 0.1 % resolution
- Beam attenuation Coefficient @ 0.1 m^{-1} resolution
- Volume concentration @ 0.1 µl/l resolution
- Volume scattering function (VSF)

The measuring of the above parameters give important information about the number, the size and the quality (phytoplankton, sediment etc) of suspended materials in the water column. Additionally, further information for the determination of the water masses is provided by the estimation of the inherent optical properties. Finally, for the first ~ 100m we could estimate the

sea color and compare this estimation to that of satellite images, helping thus to calibrate the satellite algorithms.
For the cruise MSM 72 the existence of the above optical estimations is important by itself because it is the first time that LISST – DEEP is deployed to record data in a transect across the full length of the Mediterranean Sea. Furthermore, the estimation of these parameters combined with POC - PON estimation, other chemical parameters and the CTD results, strengthen the dynamic analysis of the Mediterranean Sea.

Methods

In general the use of LISST – DEEP during the cruise follows the standard methods which are provided by Sequoia Inc, but with one important difference. For the estimation of the above parameters the use of a background file is required for normalization purposes. This file is normally produced in laboratory conditions with mili – q 2 filtered water. However, experience until now has proved that especially in the eastern Mediterranean Sea (which is characterized as ultra-oligotrophic) the use of this background file leads us to an overestimation of the parameters and especially of the beam attenuation coefficient. So, in this cruise we used a sampled in situ background file chosen as the minimum of the sum of the digital counts in the 32 rings and where the LaserPower to LaserReference (Lp/Lr) ratio is maximum.

Problems faced

The main problem which we faced during the cruise was the frequent change of the CTD main unit and the different cables that we had to use for the instrument connection to the CTD. Fortunately, with the most valuable help of the cruise technician we managed to deploy the LISST – DEEP as much as possible.
Additionally, the maximum depth limitation of the instrument (3000m) enforced us to remove it in deeper casts.

Statistics

54 stations were sampled (see figure 5.9.1)

Fig. 5.9.1 Map of the LISST stations

Data Quality

Primary data were recovered with the use of LISST-SOV-5 and processed with dedicated MATLAB routines. Overall the data quality is very good. Only exception is the median diameter (D50) estimation at casts, which are deeper than 2000m. It seems that in these casts the parameter of median diameter is overestimated. Most possibly due to the increased pressure, the shape of some of the instruments optical receivers changes. We are already in contact with Sequoia Inc, and it seems that we have found a solution to overcome this overestimation. This will allow the removal of erroneous values due to the pressure effect and the re-evaluation of particle size at large depths.
First results are shown in figure 5.9.2.

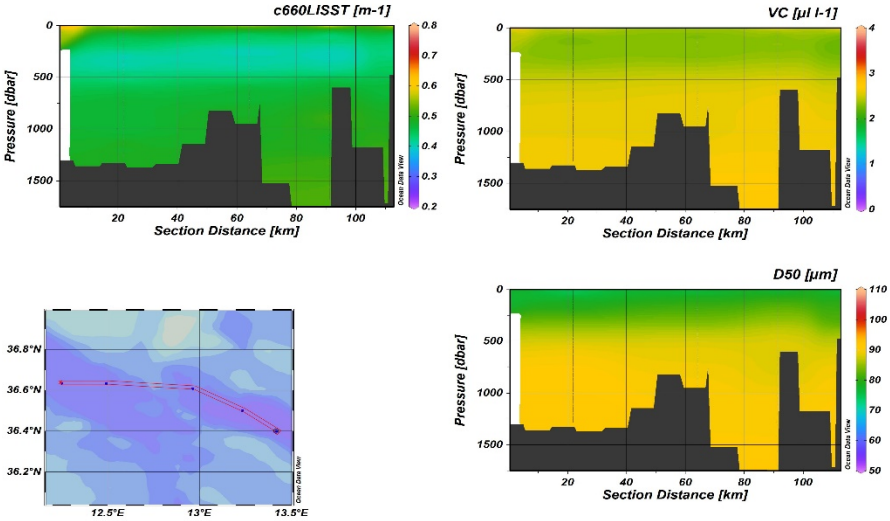

Fig. 5.9.2 Section in Sicily straight (st.68 - 73). Beam attenuation coefficient estimation, Volume concentration estimation, and median diameter estimation.

5.10. POC, PN and their stable isotopes

(Alexandra Gogou, Spyridon Chaikalis)

Biotic processes that form, change, transport, and remineralize particulate organic carbon are central to the ocean's geochemical cycling are of fundamental importance to the ocean carbon cycle. Particulate matter is mostly generated in the ocean's surface layers through primary production and a fraction is exported downward to the deep sea. During its transit towards the sea floor, most particulate organic carbon (POC) is returned to inorganic form and redistributed in the water column. This redistribution determines the surface concentration of dissolved CO2, and hence the rate at which the ocean can absorb CO2 from the atmosphere. The ability to predict quantitatively the depth profile of POC remineralization is therefore critical to predicting the response of the carbon cycle to global change.
Furthermore, the collected POC, PN and table isotope dataset collected during the MSM72 cruise will be used to identify mechanisms governing particle production, transport and cycling, aiming to obtain insight on the prevailing biogeochemical (e.g. depths of autotrophic production vs. heterotrophic consumption, marine vs. terrestrial sources) and oceanographic conditions (water mass characteristics, mixing vs. stratification, intermediate and deep water oxygenation etc) in the various Mediterranean sites.

Methodology

The study of organic carbon, nitrogen and their stables isotopes was conducted in 15 stations (100 seawater samples) along an east –west transect. For the determination of POC and PN concentrations, 5-20 L - depending on the suspended matter concentration - were collected and filtered through pre-combusted (450º C; 8h), pre-weighed 47 mm diameter, 0.7 µm particle retention GF/F filters and were stored at -20°C in the dark. Before the end of the cruise, the samples were dried in the oven at 30ºC, and have been transported to the lab.
In the lab, filters will be sealed in a desiccator and exposed to vapor from a concentrated solution of hydrochloric acid for >18 h, and after that they will be packaged into silver cups and analyzed for C and N content and stable isotopic composition at a Stable Isotope Facility using elemental analyzer interfaced with an isotope ratio mass spectrometer.

5.11. NO_3^- isotopes ($\delta^{15}N$ & $\delta^{18}O$)

(François Fripiat)

Samples for nitrogen (N) and oxygen (O) isotopes in nitrate (NO_3^-) and nitrate+nitrite ($NO_3^- + NO_2^-$) analysis were collected at 44 stations evenly distributed along the transect. In total, 790 samples have been collected. High-resolution NO_3^- $\delta^{15}N$ and $\delta^{18}O$ measurements represent a powerful tool to unravel the sources and sinks of reactive (i.e., fixed) N at the scale of the Mediterranean Sea. Complemented with coral-bound $\delta^{15}N$ records covering the last centuries, these measurements may also shed light on the contribution of industrially fixed N to the reactive N budget, by revealing the large-scale systematics required to interpret the records back in time.
Unfiltered samples for N and O isotopic composition of NO_3^- were collected in 60 mL plastic bottles and stored frozen (-20°C) until analysis. $NO_3^-+NO_2^-$ $\delta^{15}N$ and $\delta^{18}O$ will be measured (2019-2020) at the Max Planck Institute using the denitrifier method (Sigman et al., 2001; Casciotti et al., 2002). Briefly, 3-20 nmol of $NO_3^-+NO_2^-$ is quantitatively converted to N_2O gas by denitrifying bacteria (*Pseudomonas aureofaciens*) that lack an active N_2O reductase. The N_2O is then analysed by gas chromatography-isotope ratio mass spectrometer (GC-IRMS; MAT253, Thermo) with on-line cryo-trapping (Weigand et al., 2016). Measurements are referenced to air N_2 for $\delta^{15}N$ and VSMOW for $\delta^{18}O$ using the nitrate reference materials IAEA-NO3 and USGS-34. For NO_3^- $\delta^{15}N$ and $\delta^{18}O$ analysis, NO_2^- is removed with the sulfamic acid method prior to the isotopic analysis (Granger and Sigman, 2009). The reproducibility is generally better than 0.1‰ for $\delta^{15}N$ and $\delta^{18}O$, respectively.

7 Station List MSM72/1

7.1 Overall Station List

Station No.			Date	Gear	Time	Position		Water Depth	Type of Samples	Remarks
						Latitude	Longitude			
XPO-COD	No.	Cast	2018		[UTC]	[°N]	[°W/°E]	[m]		
MSM72	001	1	02.03	CTD/lADCP	20:31	35° 24,008’	026° 20,029’	289	CHE1	
MSM72	002	1	02.03	CTD/lADCP	23:26	35° 40,019’	026° 17,033’	2282	CHE2	
MSM72	002	2	03.03	CTD	2:12	35° 40,019’	026° 17,033’	2284		
MSM72	002	3	03.03	CTD/LISST	4:00	35° 40,018’	026° 17,036’	2288		
MSM72	003	1	03.03	CTD/lADCP	6:07	35° 29,016’	026° 28,041’	1034	PHY	
MSM72	004	1	03.03	CTD/lADCP	8:25	35° 18,013’	026° 39,042’	1095	CHE1	
MSM72	005	1	03.03	CTD/lADCP	10:29	35° 10,504’	026° 31,044’	686	PHY	
MSM72	006	1	03.03	CTD/lADCP	12:16	35° 06,458’	026° 21,975’	269	CHE1	
MSM72	007	1	03.03	CTD/lADCP/LISST	14:08	34° 58,103’	026° 16,521’	1592	PHY	
MSM72	008	1	03.03	CTD/lADCP/LISST	16:13	34° 48,043’	026° 09,842’	1318	CHE1	
MSM72	009	1	03.03	CTD/lADCP	20:38	34° 22,001’	025° 57,541’	3997	CHE2	
MSM72	009	2	03.03	CTD	23:41	34° 21,965’	025° 57,556’	3996		
MSM72	010	1	04.03	CTD/lADCP	2:53	34° 15,988’	025° 37,519’	2584	PHY	
MSM72	011	1	04.03	CTD/lADCP	6:35	34° 14,394’	025° 18,023’	3825	CHE1	
MSM72	011	2	04.03	CTD	9:23	34° 14,321’	025° 18,166’	3835		
MSM72	012	1	04.03	CTD/lADCP	14:23	34° 14,120’	024° 56,916’	3470	PHY	
MSM72	013	1	04.03	CTD/lADCP	19:09	34° 16,135’	024° 36,142’	3297	CHE1	
MSM72	013	1	04.03	Float ARVOR I	20:39	34° 16,199’	024° 36,203’	3224		
MSM72	013	2	04.03	Drifter DWS	20:57	34° 15,469’	024° 35,288’	2908		
MSM72	014	1	04.03	CTD/lADCP/LISST	23:53	34° 25,016’	024° 15,010’	2325	PHY	
MSM72	015	1	05.03	CTD/lADCP	3:55	34° 34,815’	023° 54,012’	2781	CHE1	
MSM72	015	1	05.03	uCTD	6:25	34° 43,126’	023° 43,597’			
MSM72	016	1	05.03	CTD/lADCP	9:11	34° 51,514’	023° 33,010’	3011	PHY	
MSM72	016	2	05.03	uCTD	11:34	34° 57,262’	023° 22,038’	2958		
MSM72	017	1	05.03	CTD/lADCP	14:10	023°12,01’	023° 12,017’	3201	CHE1	
MSM72	017	3	05.03	uCTD	16:16	35° 00,128’	023° 04,798’			
MSM72	018	1	05.03	CTD/lADCP	18:35	34° 57,308’	022° 56,028’	3241	PHY	
MSM72	018	4	05.03	uCTD	21:38	35° 08,864’	023° 07,394’	3753		
MSM72	019	1	06.03	CTD/lADCP	0:58	35° 21,000’	023° 19,023’	3184	CHE1	no bottle closing
MSM72	019	2	06.03	CTD	12:12	35° 21,003’	023° 19,025’	3176		no bottle closing
MSM72	019	3	06.03	CTD	15:49	35° 21,003’	023° 19,012’	3429		Canceling, defective CTD
MSM72	019	5	06.03	uCTD	19:58	35° 29,229’	023° 19,303’	2178		
MSM72	020	1	06.03	CTD/lADCP	22:13	35° 39,015’	023° 20,024’	419	PHY	
MSM72	020	6	07.03	uCTD	0:28	35° 38,973’	023° 04,407’	1892		
MSM72	021	1	07.03	CTD/lADCP	3:07	35° 40,023’	022° 55,011’	2965	CHE1	
MSM72	022	7	07.03	uCTD	4:37	35° 39,870’	022° 55,036’	2964		
MSM72	022	8	07.03	uCTD	5:46	35° 32,374’	022° 55,776’	2066		
MSM72	022	9	07.03	uCTD	6:46	35° 25,958’	022° 56,399’	3470		
MSM72	022	10	07.03	uCTD	7:46	35° 19,812’	022° 56,949’	3626		
MSM72	022	11	07.03	uCTD	8:48	35° 13,127’	022° 57,609’	3537		
MSM72	022	12	07.03	uCTD	9:48	35° 06,923’	022° 58,278’	3058		

MSM72	022	13	07.03	uCTD	10:53	35° 00,204'	022° 59,309'	3488		no data recorded
MSM72	022	14	07.03	uCTD	11:50	34° 54,122'	022° 59,371'	3185		
MSM72	022	15	07.03	uCTD	12:53	34° 48,189'	022° 57,892'	2964		
MSM72	022	16	07.03	uCTD	13:44	34° 48,698'	022° 53,095'	2947		
MSM72	022	1	07.03	CTD/lADCP	15:27	34° 48,843'	022° 51,444'	2944	CHE1	new CTD configuration
MSM72	022	17	07.03	uCTD	17:31	34° 49,481'	022° 44,416'	2913		
MSM72	022	18	07.03	uCTD	18:30	34° 50,032'	022° 38,098'	2906		
MSM72	022	19	07.03	uCTD	19:30	34° 50,685'	022° 32,570'	2938		
MSM72	022	20	07.03	uCTD	20:30	34° 51,348'	022° 26,895'	2992		
MSM72	022	21	07.03	uCTD	21:30	34° 51,743'	022° 20,618'	3047		
MSM72	022	22	07.03	uCTD	22:30	34° 52,403'	022° 14,853'	3098		
MSM72	022	23	07.03	uCTD	23:30	34° 52,809'	022° 08,485'	3132		
MSM72	022	24	08.03	uCTD	0:31	34° 53,704'	022° 02,174'	3298		

Station No.			**Date**	**Gear**	**Time**	**Position**		**Water Depth**	**Type of Samples**	**Remarks**
						Latitude	**Longitude**			
XPO-COD	**No.**	**Cast**	**2018**		**[UTC]**	**[°N]**	**[°W/°E]**	**[m]**		
MSM72	022	25	08.03	uCTD	1:31	34° 54,344'	021° 55,913'	3145		
MSM72	022	26	08.03	uCTD	2:28	34° 55,030'	021° 50,167'	3157		
MSM72	022	27	08.03	uCTD	3:32	34° 55,714'	021° 43,348'	3133		
MSM72	022	28	08.03	uCTD	4:29	34° 56,354'	021° 37,547'	3257		
MSM72	022	29	08.03	uCTD	5:27	34° 57,015'	021° 31,588'	3267		
MSM72	022	30	08.03	uCTD	6:30	34° 57,754'	021° 24,631'	2899		
MSM72	022	31	08.03	uCTD	7:30	34° 57,845'	021° 19,067'	2633		
MSM72	022	32	08.03	uCTD	8:30	34° 58,487'	021° 14,311'	2733		
MSM72	022	33	08.03	uCTD	9:28	35° 01,889'	021° 04,678'	2738		
MSM72	022	34	08.03	uCTD	11:00	35° 01,889'	021° 04,678'	2738		
MSM72	022	35	08.03	uCTD	12:01	35° 04,387'	021° 09,788'	2860		
MSM72	022	36	08.03	uCTD	12:59	35° 06,651'	021° 14,287'	2816		
MSM72	022	37	08.03	uCTD	14:05	35° 08,837'	021° 19,654'	3107		
MSM72	023	1	08.03	CTD/lADCP	22:45	35° 40,992'	022° 28,015'	4524	CHE1	
MSM72	023	38	09.03	uCTD	2:07	35° 40,466'	022° 42,414'	0		
MSM72	024	1	09.03	CTD/lADCP	4:32	35° 39,989'	022° 55,027'	2969	CHE1	
MSM72	024	39	09.03	uCTD	6:38	35° 47,000'	022° 58,292'	1842		
MSM72	025	1	09.03	CTD/lADCP	8:36	35° 54,990'	023° 02,028'	1049	PHY	
MSM72	025	40	09.03	uCTD	10:39	35° 57,879'	022° 45,088'	1163		
MSM72	026	1	09.03	CTD/lADCP	13:13	35° 59,993'	022° 32,024'	3167	CHE1	
MSM72	026	41	09.03	uCTD	15:27	36° 07,090'	022° 31,180'	2792		
MSM72	027	1	09.03	CTD/lADCP	17:31	36° 14,986'	022° 30,029'	2166	PHY	
MSM72	027	42	09.03	uCTD	20:17	36° 15,492'	022° 06,983'	2713		
MSM72	028	1	10.03	CTD/lADCP	0:02	36° 15,809'	021° 42,499'	3571	CHE1	
MSM72	029	43	10.03	uCTD	1:45	36° 16,011'	021° 42,555'	3539		
MSM72	029	44	10.03	uCTD	2:45	36° 22,209'	021° 44,487'	3551		
MSM72	029	45	10.03	uCTD	3:44	36° 27,591'	021° 45,995'	3093		
MSM72	029	46	10.03	uCTD	4:43	36° 33,464'	021° 47,564'	2427		
MSM72	029	47	10.03	uCTD	5:43	36° 32,959'	021° 48,632'	2280		
MSM72	029	48	10.03	uCTD	6:45	36° 26,914'	021° 49,855'	2488		
MSM72	029	49	10.03	uCTD	7:47	36° 20,742'	021° 51,043'	3744		
MSM72	029	50	10.03	uCTD	9:17	36° 13,660'	021° 52,271'	3545		
MSM72	029	51	10.03	uCTD	10:14	36° 08,564'	021° 53,432'	3160		
MSM72	029	52	10.03	uCTD	11:15	36° 05,966'	021° 48,443'	3886		
MSM72	029	53	10.03	uCTD	12:14	36° 06,015'	021° 41,212'	3567		
MSM72	029	54	10.03	uCTD	13:15	36° 06,027'	021° 33,438'	3607		
MSM72	029	55	10.03	uCTD	14:14	36° 06,004'	021° 25,814'	3693		
MSM72	029	56	10.03	uCTD	15:14	36° 08,009'	021° 19,984'	3972		
MSM72	029	57	10.03	uCTD	16:13	36° 13,914'	021° 19,993'	4352		
MSM72	029	58	10.03	uCTD	17:14	36° 20,172'	021° 20,053'	4312		
MSM72	029	59	10.03	uCTD	18:12	36° 25,947'	021° 19,997'	4213		
MSM72	30	1	10.03	CTD/lADCP	20:25	36° 30,042'	021° 20,025'	4233	CHE1	
MSM72	30	60	11.03	uCTD	0:04	36° 44,697'	021° 05,365'	3919		
MSM72	31	1	11.03	CTD/lADCP	3:15	36° 58,486'	020° 51,618'	2578	PHY	
MSM72	31	61	11.03	uCTD	5:43	37° 09,676'	020° 36,886'	2595		

MSM72	32	1	11.03	CTD/lADCP	9:18	37° 22,511’	020° 20,030’	4250	CHE1	
MSM72	32	3	11.03	Float AVOR I	11:04	37° 22,506’	020° 20,031’	4240		
MSM72	32	62	11.03	uCTD	13:08	37° 40,883’	020° 17,378’	2714		
MSM72	33	1	11.03	CTD/lADCP/LISST	15:34	37° 57,621’	020° 15,026’	811	PHY	
MSM72	33	63	11.03	uCTD	17:29	38° 11,122’	020° 08,073’	3400		
MSM72	34	1	11.03	CTD/lADCP	20:12	38° 23,918’	020° 01,535’	2603	CHE2	
MSM72	34	2	11.03	CTD	22:35	38° 23,920’	020° 01,534’	2604		
MSM72	34	4	11.03	Float PROV-BIO	22:51	38° 23,918’	020° 01,538’	2600		
MSM72	34	64	12.03	ucCTD	0:38	38° 38,072’	019° 54,189’	1922		
MSM72	35	1	12.03	CTD/lADCP	2:55	38° 50,111’	019° 47,990’	1448	PHY	
MSM72	35	65	12.03	ucCTD	4:50	39° 02,029’	019° 43,222’	1444		
MSM72	36	1	12.03	CTD/lADCP	7:11	39° 15,043’	019° 38,021’	1404	CHE1	
MSM72	36	66	12.03	ucCTD	9:22	39° 27,162’	019° 33,112’	1253		
MSM72	37	1	12.03	CTD/lADCP	11:26	39° 40,222’	019° 27,885’	346	PHY	

Station No.			Date	Gear	Time	Position		Water Depth	Type of Samples	Remarks
						Latitude	Longitude			
XPO-COD	No.	Cast	2018		[UTC]	[°N]	[°W/°E]	[m]		
MSM72	37	67	12.03	ucCTD	12:54	39° 49,228’	019° 19,903’	823		
MSM72	38	1	12.03	CTD/lADCP	14:25	39° 56,025’	019° 16,994’	987	CHE1	
MSM72	38	68	12.03	uCTD	15:44	40° 02,085’	019° 18,202’	996		
MSM72	39	1	12.03	CTD/lADCP/LISST	17:24	40° 10,237’	019° 19,831’	935	PHY	
MSM72	40	1	12.03	CTD/lADCP/LISST	19:27	40° 10,232’	019° 10,217’	969	CHE1	
MSM72	41	1	12.03	CTD/lADCP/LISST	21:36	40° 10,222’	019° 00,045’	926	PHY	
MSM72	42	1	12.03	CTD/lADCP/LISST	23:34	40° 10,223’	018° 49,788’	777	CHE1	
MSM72	43	1	13.03	CTD/lADCP/LISST	1:22	40° 10,229’	018° 43,016’	598	PHY	
MSM72	43	69	13.03	uCTD	4:18	39° 49,705’	018° 58,653’	904		
MSM72	43	70	13.03	uCTD	6:18	39° 36,106’	019° 08,904’	1082		
MSM72	43	71	13.03	uCTD	8:13	39° 22,396’	019° 19,285’	1168		
MSM72	43	72	13.03	uCTD	10:16	39° 07,414’	019° 30,607’	1102		
MSM72	43	73	13.03	uCTD	12:15	38° 52,918’	019° 41,961’	1341		
MSM72	43	74	13.03	uCTD	14:14	38° 38,660’	019° 52,648’	1762		
MSM72	43	75	13.03	uCTD	16:13	38° 24,230’	020° 03,409’	2685		
MSM72	43	76	13.03	uCTD	18:12	38° 09,169’	020° 11,644’	2505		
MSM72	43	77	13.03	uCTD	20:14	37° 54,040’	020° 23,862’	1599		
MSM72	43	78	13.03	uCTD	22:15	37° 39,699’	020° 35,585’	1129		
MSM72	43	79	14.03	uCTD	0:14	37° 25,669’	020° 45,781’	3362		
MSM72	43	80	14.03	uCTD	4:13	36° 53,692’	021° 09,335’	2016		
MSM72	43	81	14.03	uCTD	6:16	36° 39,668’	021° 22,171’	4108		
MSM72	43	82	14.03	uCTD	8:13	36° 26,328’	021° 33,766’	3898		
MSM72	44	1	14.03	CTD/lADCP	17:18	35° 02,016’	022° 40,019’	3154	CHE1	
MSM72	44	83	14.03	uCTD	19:32	35° 03,141’	022° 31,015’	3347		
MSM72	45	1	14.03	CTD/lADCP	21:53	35° 04,628’	022° 20,009’	3321	PHY	
MSM72	45	84	14.03	uCTD	23:45	35° 05,824’	022° 10,493’	3186		
MSM72	46	1	15.03	CTD/lADCP	1:59	35° 07,230’	021° 59,410’	3247	CHE1	
MSM72	46	85	15.03	uCTD	4:25	35° 10,719’	021° 44,345’	3304		
MSM72	47	1	15.03	CTD/lADCP	6:23	35° 14,319’	021° 28,850’	3514	CHE2	
MSM72	47	2	15.03	CTD/lADCP	9:46	35° 14,394’	021° 28,850’	3528	CHE2	
MSM72	47	86	15.03	uCTD	12:04	35° 11,648’	021° 14,156’	3096		
MSM72	48	1	15.03	CTD/lADCP	14:27	35° 08,992’	021° 00,050’	3078	PHY	
MSM72	48	87	15.03	uCTD	16:10	35° 07,853’	020° 50,846’	2806		
MSM72	49	1	15.03	CTD/lADCP/LISST	18:13	35° 06,588’	020° 14,523’	2851	CHE1	
MSM72	49	88	15.03	uCTD	20:12	35° 05,528’	020° 31,758’	2958		
MSM72	50	1	15.03	CTD/lADCP/LISST	22:22	35° 04,234’	020° 21,014’	2996	PHY	
MSM72	50	5	15.03	Drifter	23:24	35° 04,189’	020° 20,990’	3237		
MSM72	50	89	16.03	uCTD	0:31	35° 07,565’	020° 06,521’	2958		
MSM72	51	1	16.03	CTD/lADCP	2:55	35° 10,760’	019° 53,219’	2975	CHE1	
MSM72	51	90	16.03	uCTD	4:57	35° 13,510’	019° 41,652’	3176		
MSM72	52	1	16.03	CTD/lADCP	7:38	35° 17,143’	019° 25,474’	3368.7	CHE1	
MSM72	52	91	16.03	uCTD	6:37	35° 17,145’	019° 25,473’	3369		
MSM72	53	1	16.03	CTD/lADCP	12:55	35° 23,621’	018° 57,818’	3771	CHE1	
MSM72	53	92	16.03	uCTD	15:32	35° 27,785’	018° 44,951’	3918		
MSM72	54	1	16.03	CTD/lADCP	18:32	35° 29,658’	018° 29,959’	4018	PHY	

MSM72	54	6	16.03	Float	19:59	35° 29,341'	018° 29,951'	4016		
MSM72	54	7	16.03	Drifter	20:09	35° 28,541'	018° 30,037'	4284		
MSM72	54	93	16.03	uCTD	20:49	35° 24,683'	018° 23,038'	3908		
MSM72	55	1	16.03	CTD/lADCP	23:32	35° 18,002'	018° 11,991'	3862	CHE2	
MSM72	55	2	17.03	CTD/lADCP	2:30	35° 17,996'	018° 11,995'	3866	CHE2	
MSM72	56	1	17.03	CTD/lADCP	6:10	35° 06,020'	017° 53,992'	3576	PHY	
MSM72	57	1	17.03	CTD/lADCP	10:45	34° 54,048'	017° 35,988'	2950	CHE1	
MSM72	58	1	17.03	CTD/lADCP	15:15	34° 42,006'	017° 18,011'	2831	PHY	
MSM72	59	1	17.03	CTD/lADCP/LISST	19:32	34° 50,995'	016° 48,006'	2292	CHE1	
MSM72	59	94	17.03	uCTD	21:53	34° 55,376'	016° 33,362'	2086		
MSM72	60	1	18.03	CTD/lADCP	0:16	35° 00,009'	016° 17,985'	1497	PHY	
MSM72	61	1	18.03	CTD/lADCP	4:18	35°18,864'	015° 49,829'	413	CHE1	
MSM72	62	1	18.03	CTD/lADCP/LISST	7:53	35°37,786'	015° 21,641'	284	PHY	
MSM72	63	1	18.03	CTD/lADCP	11:48	35°37,920'	014° 45,780'	134	CHE1	

Station No.			**Date**	**Gear**	**Time**	**Position**		**Water Depth**	**Type of Samples**	**Remarks**
						Latitude	**Longitude**			
XPO-COD	**No.**	**Cast**	**2018**		**[UTC]**	**[°N]**	**[°W/°E]**	**[m]**		
MSM72	64	1	18.03	CTD/lADCP	15:26	35°38,028'	014° 10,025'	556	PHY	
MSM72	64	95	18.03	uCTD	17:38	35° 43,562'	013° 45,671'	601,8		
MSM72	64	96	18.03	uCTD	20:02	35° 48,069'	013° 18,644'	1446		
MSM72	65	1	18.03	CTD/lADCP	22:52	35°49,965'	013° 05,074'	1530	PHY	
MSM72	65	97	18.03	uCTD	23:36	35° 50,143'	013° 05,354'	1533		
MSM72	66	1	19.03	CTD/lADCP	3:30	36° 00,995'	013° 47,503'	1111	CHE1	
MSM72	66	98	19.03	uCTD	4:45	36° 06,896'	013° 44,004'	1036		
MSM72	67	1	19.03	CTD/lADCP	6:23	36° 12,990'	013° 38,976'	1308	PHY	
MSM72	67	99	19.03	uCTD	7:44	36° 18,722'	013° 31,740'	1265		
MSM72	68	1	19.03	CTD/lADCP/LISST	9:35	36° 23,981'	013° 25,032'	1710	CHE2	
MSM72	68	100	19.03	uCTD	11:03	36° 26,885'	013° 19,663'	1722		
MSM72	69	1	19.03	CTD/lADCP/LISST	12:36	36° 30,018'	013° 13,981'	1713	PHY	
MSM72	69	101	19.03	uCTD	14:05	36° 33,803'	013° 04,473'	1214		
MSM72	70	1	19.03	CTD/lADCP/LISST	15:35	36° 36,494'	012° 57,798'	1013	CHE1	
MSM72	70	102	19.03	uCTD	16:48	36° 36,860'	012° 50,504'	785,5		
MSM72	70	103	19.03	uCTD	18:00	36° 37,485'	012° 38,783'	1193		
MSM72	71	1	19.03	CTD/lADCP/LISST	19:55	36° 37,985'	012° 29,520'	1311	PHY	
MSM72	71	104	19.03	uCTD	21:13	36° 39,242'	012° 23,235'	1316		
MSM72	72	1	19.03	CTD/lADCP	23:16	36° 38,022'	012° 15,030'	1302	CHE1	
MSM72	72	105	20.03	uCTD	0:17	36° 38,387'	012° 14,986'	1304		
MSM72	72	106	20.03	uCTD	2:03	36° 48,949'	012° 12,009'	1163		
MSM72	73	1	20.03	CTD/lADCP/LISST	7:09	37° 21,324'	012° 03,011'	77	CHE1	
MSM72	74	1	20.03	CTD/lADCP/LISST	10:20	37° 32,017'	012° 22,087'	80	PHY	
MSM72	75	1	21.03	CTD/lADCP	7:38	39° 10,948'	013° 30,066'	3096	CHE1	Bottles did not close, CTD probes changed
MSM72	75	2	21.03	CTD/lADCP	12:14	39° 10,948'	013° 30,066'	3100	CHE1	
MSM72	75	7	21.03	Float	14:42	39° 10,948	013° 30,06'	3083		
MSM72	75	107	21.03	uCTD	15:56	39° 11,983'	013° 10,128'	3152		
MSM72	76	1	21.03	CTD/lADCP	18:44	39° 13,000	012° 50,029'	3418	PHY	
MSM72	76	108	21.03	uCTD	22:04	39° 13,036'	012° 29,529'	3170		
MSM72	76	109	22.03	uCTD	22:04	39° 13,110'	012° 05,920'	3100		
MSM72	77	1	22.03	CTD/lADCP	2:17	39° 13,198'	011° 45,042'	3218	CHE2	
MSM72	77	2	22.03	CTD/lADCP	4:49	39° 13,010'	011° 44,992'	3155	CHE2	
MSM72	77	8	22.03	Float	6:08	39° 12,950'	011° 44,96'	3200		
MSM72	78	110	22.03	uCTD	6:21	39° 12,704'	011° 44,929'	3056		
MSM72	78	111	22.03	uCTD	7:27	39° 05,312'	011° 44,070'	2552		
MSM72	78	112	22.03	uCTD	8:33	38° 58,086'	011° 43,278'	2284		
MSM72	78	113	22.03	uCTD	9:40	38° 50,784'	011° 42,289'	1859		
MSM72	78	114	22.03	uCTD	10:57	38° 42,283'	011° 41,445'	1933		
MSM72	78	115	22.03	uCTD	12:25	38° 31,965'	011° 41,040'	2512		
MSM72	78	116	22.03	uCTD	13:59	38° 21,813'	011° 38,655'	1071		
MSM72	78	117	22.03	uCTD	15:19	38° 12,334'	011° 37,984'	713,1		
MSM72	78	118	22.03	uCTD	16:32	38° 02,816'	011° 36,797'	708,9		
MSM72	79	1	22.03	CTD/lADCP/LISST	18:11	37° 53,539'	011° 35,558'	474	CHE1	
MSM72	80	1	22.03	CTD/lADCP	21:21	38° 06,366'	011° 20,776'	500	PHY	
MSM72	81	1	23.03	CTD/lADCP	0:10	38° 19,334'	011° 6,106'	712	CHE1	

MSM72	82	1	23.03	CTD/lADCP	3:08	38° 32,213’	010° 51,523’	717	PHY	
MSM72	83	1	23.03	CTD/lADCP/LISST	6:23	38° 44,977’	010° 36,634’	2469	CHE1	
MSM72	83	2	23.03	CTD/lADCP/LISST	8:44	38° 44,976’	010° 36,631’	2598	CHE1	
MSM72	83	119	23.03	uCTD	11:12	38° 43,878’	010° 22,921’	2690		
MSM72	83	120	23.03	uCTD	12:41	38° 42,870’	010° 09,675’	2110		
MSM72	84	1	23.03	CTD/lADCP/LISST	14:48	38° 42,007’	009° 59,026’	2270	PHY	
MSM72	84	121	23.03	uCTD	16:49	38° 36,329’	009° 48,143’	2061		
MSM72	85	1	23.03	CTD/lADCP/LISST	18:49	38° 30,997’	009° 38,543’	1866	CHE1	
MSM72	85	122	23.03	uCTD	19:53	38° 30,919’	009° 38,023’	1869		
MSM72	85	123	23.03	uCTD	21:25	38° 24,087’	009° 26,078’	1630		
MSM72	86	1	23.03	CTD/lADCP	23:22	38° 19,982’	009° 18,023’	1927	PHY	
MSM72	86	124	24.03	uCTD	1:05	38° 19,242’	009° 07,590’	1991		
MSM72	87	1	24.03	CTD/lADCP	2:58	38° 18,476’	008° 58,525’	2107	CHE1	
MSM72	87	125	24.03	uCTD	4:43	38° 17,771’	008° 48,827’	2178		

Station No.			**Date**	**Gear**	**Time**	**Position**		**Water Depth**	**Type of Samples**	**Remarks**
						Latitude	**Longitude**			
XPO-COD	**No.**	**Cast**	**2018**		**[UTC]**	**[°N]**	**[°W/°E]**	**[m]**		
MSM72	88	1	24.03	CTD/lADCP	6:41	38° 17,005’	008° 39,030’	2124	PHY	
MSM72	88	126	24.03	uCTD	7:35	38° 17,143’	008° 38,765’	2120		
MSM72	88	127	24.03	uCTD	9:03	38° 22,224’	008° 27,131’	816,5		
MSM72	89	1	24.03	CTD/lADCP/LISST	10:54	38° 25,526’	008° 19,529’	2112	CHE1	
MSM72	89	128	24.03	uCTD	12:55	38° 29,908’	008° 09,380’	2242		
MSM72	90	1	24.03	CTD/lADCP/LISST	14:56	38° 34,080’	008° 00,128’	2214	PHY	
MSM72	90	129	24.03	uCTD	16:48	38° 39,141’	007° 50,009’	2381		
MSM72	91	1	24.03	CTD/lADCP/LISST	18:24	38° 44,312’	007° 40,483’	2829	CHE2	
MSM72	91	2	24.03	CTD/lADCP/LISST	21:04	38° 44,302’	007° 40,453’	2836	CHE2	
MSM72	91	130	24.03	uCTD	22:28	38° 44,480’	007° 40,145’	2835		
MSM72	91	131	25.03	uCTD	0:00	38° 50,270’	007° 28,640’	2841		
MSM72	92	1	25.03	CTD/lADCP	2:11	38° 54,515’	007° 21,012’	2843	PHY	
MSM72	92	132	25.03	uCTD	3:57	38° 56,455’	007° 11,260’	2850		
MSM72	93	1	25.03	CTD/lADCP	6:06	38° 57,348’	007° 01,506’	2849	CHE1	
MSM72	93	133	25.03	uCTD	8:20	38° 58,863’	006° 51,977’	2849		
MSM72	94	1	25.03	CTD/lADCP/LISST	10:31	39°00,090’	006° 41,934’	2852	PHY	
MSM72	94	134	25.03	uCTD	11:39	38° 59,932’	006° 41,403’	2853		
MSM72	94	135	25.03	uCTD	12:54	38° 58,058’	006° 31,076’	2857		
MSM72	95	1	25.03	CTD/lADCP/LISST	14:49	39°56,808’	006° 24,612’	2865	CHE1	
MSM72	95	136	25.03	uCTD	16:39	38° 55,832’	006° 17,188’	2863		
MSM72	96	1	25.03	CTD/lADCP/LISST	18:52	38°53,934’	006° 07,194’	2857	PHY	
MSM72	96	137	25.03	uCTD	20:38	38° 52,754’	005° 58,727’	2857		
MSM72	97	1	25.03	CTD/lADCP/LISST	22:08	38°50,974’	005° 49,816’	2851	CHE2	
MSM72	97	2	26.03	CTD/lADCP/LISST	0:38	38°50,971’	005° 49,814’	2850	CHE2	
MSM72	97	138	26.03	uCTD	1:55	38° 50,973’	005° 49,419’	2843		
MSM72	97	139	26.03	uCTD	2:58	38° 50,009’	005° 40,419’	2851		
MSM72	98	1	26.03	CTD/lADCP	4:58	38°47,982’	005° 32,395’	2846	PHY	
MSM72	98	140	26.03	uCTD	6:44	38° 47,163’	005° 23,256’	2836		
MSM72	99	1	26.03	CTD/lADCP	8:57	38°44,976’	005° 15,020’	2803	CHE1	
MSM72	99	141	26.03	uCTD	11:08	38° 43,448’	005° 05,206’	2801		
MSM72	100	1	26.03	CTD/lADCP/LISST	13:09	38°42,008’	004° 57,640’	2742	PHY	
MSM72	100	142	26.03	uCTD	14:09	38° 41,981’	004° 57,476’	2733		
MSM72	100	143	26.03	uCTD	15:23	38° 40,230’	004° 47,042’	2699		
MSM72	101	1	26.03	CTD/lADCP/LISST	17:13	38°39,008’	004° 40,254’	2652	CHE1	
MSM72	101	144	26.03	uCTD	19:11	38° 37,331’	004° 31,998’	2421		
MSM72	102	1	26.03	CTD/lADCP/LISST	21:15	38°35,969’	004° 22,820’	2476	PHY	
MSM72	102	145	26.03	uCTD	23:29	38° 34,615’	004° 10,855’	2625		
MSM72	103	1	27.03	CTD/lADCP	0:56	38° 33,000’	004° 05,090’	2541	CHE1	
MSM72	103	146	27.03	uCTD	2:05	38° 33,002’	004° 04,953’	2535		
MSM72	103	147	27.03	uCTD	3:13	38° 31,163’	003° 54,949’	2533		
MSM72	104	1	27.03	CTD/lADCP	5:03	38° 29,659’	003° 46,944’	2588	PHY	
MSM72	104	148	27.03	uCTD	6:26	38° 28,245’	003° 40,742’	2617		
MSM72	105	1	27.03	CTD/lADCP/LISST	8:14	38° 26,970’	003° 35,207’	2615	CHE1	
MSM72	105	149	27.03	uCTD	10:39	38° 25,440’	003° 22,058’	2692		
MSM72	106	1	27.03	CTD/lADCP	12:48	38° 23,996’	003° 12,047’	2704	PHY	

MSM72	106	150	27.03	uCTD	13:57	38° 24,015’	003° 11,749’	2713		
MSM72	106	151	27.03	uCTD	15:08	38° 21,232’	003° 02,185’	2723		
MSM72	107	1	27.03	CTD/lADCP/LISST	17:06	38° 19,494’	002° 54,032’	2741	CHE1	
MSM72	107	152	27.03	uCTD	19:14	38° 17,220’	002° 44,885’	2725		
MSM72	108	1	27.03	CTD/lADCP/LISST	21:23	38° 15,013’	002° 36,034’	2732	PHY	
MSM72	108	153	27.03	uCTD	23:13	38° 12,472’	002° 26,131’	2733		
MSM72	109	1	28.03	CTD/lADCP	1:14	38° 10,402’	002° 18,012’	2743	CHE1	
MSM72	109	154	28.03	uCTD	2:25	38° 10,314’	002° 17,896’	2742		
MSM72	109	155	28.03	uCTD	3:37	38° 08,051’	002° 08,035’	2190		
MSM72	110	1	28.03	CTD/lADCP	5:26	38° 06,010’	002° 00,040’	1883	PHY	
MSM72	110	156	28.03	uCTD	7:02	38° 03,423’	001° 50,740’	1791		
MSM72	111	1	28.03	CTD/lADCP/LISST	8:53	38° 01,026’	001° 42,026’	1624	CHE1	
MSM72	111	157	28.03	uCTD	10:38	37° 57,931’	001° 32,008’	2357		
MSM72	112	1	28.03	CTD/lADCP/LISST	12:32	37° 55,511’	001° 24,091’	2495	PHY	

Station No.			**Date**	**Gear**	**Time**	**Position**		**Water Depth**	**Type of Samples**	**Remarks**
						Latitude	**Longitude**			
XPO-COD	**No.**	**Cast**	**2018**		**[UTC]**	**[°N]**	**[°W/°E]**	**[m]**		
MSM72	112	158	28.03	uCTD	13:37	37° 55,435’	001° 23,924’	2500		
MSM72	112	159	28.03	uCTD	14:50	37° 52,776’	001° 13,194’	2588		
MSM72	113	1	28.03	CTD/lADCP/LISST	16:08	37° 50,490’	001° 06,073’	2637	CHE2	
MSM72	113	2	28.03	CTD/lADCP/LISST	18:24	37° 50,377’	001° 06,184’	2638	CHE2	
MSM72	113	160	28.03	uCTD	20:25	37° 48,046’	000° 56,770’	2751		
MSM72	114	1	28.03	CTD/lADCP	22:29	37° 45,498’	000° 48,014’	2764	PHY	
MSM72	114	161	29.03	uCTD	0:28	37° 39,955’	000° 38,039’	2654		
MSM72	115	1	29.03	CTD/lADCP	2:36	37° 35,514’	000° 30,010’	2676	CHE1	
MSM72	115	162	29.03	uCTD	3:47	37° 35,451’	000° 29,941’	2683		
MSM72	115	163	29.03	uCTD	5:19	37° 28,541’	000° 17,370’	2731		
MSM72	116	1	29.03	CTD/lADCP/LISST	7:01	37° 25,511’	000° 12,025’	2731	PHY	
MSM72	116	164	29.03	uCTD	8:44	37° 20,839’	000° 06,125’	2725		
MSM72	117	1	29.03	CTD/lADCP/LISST	10:44	37° 15,980’	000° 00,042’	2713	CHE1	
MSM72	117	165	29.03	uCTD	12:46	37° 12,429’	-000°08,498’	2700		
MSM72	117	166	29.03	uCTD	13:54	37° 09,149’	000° 16,457’	2687		
MSM72	118	1	29.03	CTD/lADCP/LISST	15:55	37° 06,090’	000° 23,838’	2670	PHY	
MSM72	118	167	29.03	uCTD	18:50	37° 00,148’	-000°35,730’	2666		
MSM72	119	1	29.03	CTD/lADCP/LISST	20:24	37° 57,012’	-000°41,965’	2669	CHE1	
MSM72	119	168	29.03	uCTD	22:48	36° 52,195’	-000°51,568’	2653		
MSM72	120	1	30.03	CTD/lADCP	1:00	36° 47,996’	-000°59,962’	2627	PHY	
MSM72	120	169	30.03	uCTD	3:13	36° 42,241’	-001°11,423’	2612		
MSM72	121	1	30.03	CTD/lADCP	5:16	36° 39,019’	-001°17,976’	2431	CHE1	
MSM72	121	170	30.03	uCTD	6:30	36° 38,924’	-001° 8,169’	2437		
MSM72	122	1	30.03	CTD/lADCP/LISST	9:40	36° 30,004’	-001°35,964’	1452	PHY	
MSM72	123	1	30.03	CTD/lADCP/LISST	12:59	36° 27,990’	-001°55,448’	1390	CHE1	
MSM72	124	1	30.03	CTD/lADCP/LISST	16:17	36° 27,020’	-002°14,378’	1021	PHY	
MSM72	125	1	30.03	CTD/lADCP/LISST	19:51	36° 23,315’	-002°34,472’	1382	CHE1	
MSM72	126	1	31.03	CTD/lADCP	0:33	36° 20,957’	-002°53,969’	1072	PHY	
MSM72	127	1	31.03	CTD/lADCP	4:00	36° 14,990’	-003°13,440’	845	PHY	
MSM72	128	1	31.03	CTD/lADCP	6:20	36° 05,015’	-003°13,494’	1162	CHE1	
MSM72	128	171	31.03	uCTD	8:12	36° 05,209’	-003°25,167’	729,1		
MSM72	128	172	31.03	uCTD	9:40	36° 04,382’	-003° 8,523’	784,6		
MSM72	129	1	31.03	CTD/lADCP/LISST	12:09	36° 04,982’	-003°52,427’	1177	CHE1	
MSM72	129	173	31.03	uCTD	12:55	36° 04,547’	-003°52,690’	1190		
MSM72	129	174	31.03	uCTD	14:33	36° 03,175’	-004°05,996’	1316		
MSM72	129	175	31.03	uCTD	16:23	36° 01,349’	-004°20,382’	1306		
MSM72	130	1	31.03	CTD/lADCP/LISST	18:14	36° 00,020’	-004°30,743’	1240	CHE2	for calibrating UCTD 289 and 183
MSM72	130	176	31.03	uCTD	17:54	36° 00,035’	-004°30,556’	1244		
MSM72	130	2	31.03	CTD/lADCP/LISST	19:13	36° 00,062’	-004°30,208’	1244	CHE2	
MSM72	131	1	31.03	CTD/lADCP	23:12	36° 05,358’	-004°49,661’	928	PHY	
MSM72	132	1	01.04	CTD/lADCP	2:18	35° 58,132’	-005°07,181’	516	CHE1	
MSM72	133	1	01.04	CTD/lADCP/LISST	5:58	35° 59,274’	-005°24,865’	933	PHY	
MSM72	134	1	01.04	CTD/lADCP/LISST	11:24	35° 58,656’	-005°40,134’	347	CHE1	
MSM72	135	1	01.04	CTD/lADCP/LISST	12:39	35° 56,046’	-005°40,270’	562	CHE1	
MSM72	136	1	01.04	CTD/lADCP/LISST	14:00	35° 53,233’	-005°39,755’	336	CHE1	

PHY: Stations without any chemical samples
CHE1: Stations including chemical samples
CHE2: CHE1 with additional isotope sampling

8 Data and Sample Storage and Availability

The hydrographical data will include:

- CTD data of pressure, temperature, salinity and oxygen of all CTD stations listed. The data will be calibrated before access is granted to the public.
- lADCP data of vertical velocity profiles of all CTD stations listed. The data will be calibrated before access is granted to the public.
- Underway-CTD data of pressure, temperature and salinity. The data will be calibrated before access is granted to the public.
- Continuously taken ADCP data for the whole cruise track (within diplomatic permitted areas). This data will be calibrated before access is granted to the public.
- Continuously taken thermosalinograph data. The data will be calibrated before access is granted to the public.

All data will be sent to the World Data Center "PANGAEA" which is member of the ICSU World Data System (presumably middle of 2019). This will ensure permanent availability of data to the scientific community. Since this is a cruise of the GO-SHIP programme, the hydrographic data and the bottle data will be submitted to CCHDO, https://cchdo.ucsd.edu/.
In Kiel a joint Datamanagement-Team is active, which stores the data from various projects and cruises in a web-based multi-user-system. Data gathered during MSM72 are stored at the Kiel data portal, and is proprietary for the PIs of the cruise prior to submission to open data repositories.

Table 8.1 Overview of data availability

Data	Database	Available since	Free Access	Contact
CTD	PANGAEA	April 2018	April 2019	dagmar.hainbucher@uni-amburg.de
uCTD	PANGAEA	April 2018	April 2019	dagmar.hainbucher@uni-amburg.de
ADCP	PANGAEA	April 2018	April 2019	dagmar.hainbucher@uni-amburg.de
lADCP	PANGAEA	April 2018	April 2019	dagmar.hainbucher@uni-amburg.de
Thermosalinograph	PANGAEA	April 2018	April 2019	dagmar.hainbucher@uni-amburg.de
Bottle data	PANGAEA	April 2018	April 2019	ttanhua@geomar.de
Bottle data (after analysis in the laboratory)	PANGAEA	End 2019	End 2020	ttanhua@geomar.de

9 Acknowledgements

We thank Captain Björn Maaß, his officers and the crew of R/V MARIA S. MERIAN for the support of our scientific programme, for their unending competent and friendly help. We always enjoy staying on board of R/V MERIAN.
We thank Milena Menna from OGS for providing daily Absolute Dynamic Topography maps of the Mediterranean. We thank Martin Gade from IfMHH for providing us with satellite images.
The financial support for the cruise was provided by the project of the "Deutsche Forschungsgemeinschaft" U4600DFG040204. We gratefully acknowledge their support.

10 References

Bullister, J. L., and Weiss, R. F.: Determination of CCl3F and CCl2F2 in seawater and air, Deep-Sea Res., 35, 839-853, 1988.

Byrne, R. H., Yao, W (2008). Procedures for measurement of carbonate ion concentrations in seawater by direct espectrophotometric observations of Pb(II) complexation. Mar. Chem., 112 (1−2), 128−135.

Carlson C.A. and Hansell D.A. (2015). DOM sources, sinks, reactivity, and budgets. In Biogeochemistry of Marine Dissolved Organic Matter (Second Edition) (pp. 65-126).https://doi.org/10.1016/B978-0-12-405940-5.00003-0.Carlson

Casciotti, K.L., D.M. Sigman, M. Galanter Hastings, J.K. Böhlke, and A. Hilkert. 2002. Measurement of the oxygen isotopic composition of nitrate in seawater and freshwater using the denitrifier method. Anal. Chem. 74: 4905-4912.

Clayton and Byrne (1993). Spectrophotometric seawater pH measurements: total hydrogen ion concentration scale concentration scale calibration of m-cresol purple and at-sea results. Deep-sea Research I, Vol. 40, 10, 2115-2129.

Dickson, A.G., Millero, F.J. (1987). A comparison of the equilibrium constants for the dissociation of carbonic acid in seawater media. Deep-Sea Research 34, 1733–1743.

Easley, R.A., Patsavas, M.C., Byrne, R. H., Liu, X., Feely, R.A., Mathis, J.T. (2013). Spectrophotometric measurement of calcium carbonate saturation states in seawater. Environ. Sci. Technol., 47 (3), 1468−1477.

Gonnelli, M., Galletti, Y., Marchetti, E., Mercadante, L., Retelletti Brogi, S., Ribotti, A., Sorgente R., Vestri, S. and Santinelli, C. (2016). Dissolved organic matter dynamics in surface waters affected by oil spill pollution: Results from the Serious Game exercise Deep-Sea Res. II 133: 88-99.

Granger, J., and D.M. Sigman. 2009. Removal of nitrite with sulfamic acid for nitrate N and O isotope analysis with the denitrifier method. Rapid Commun. Mass Spectrom. 23: 3753-3762, doi:10.1002/rcm.4307.

Johnson, K.M., Wills, K.D., Butler, D.B., Johnson, W.K., Wong, C.S., (1993). Coulometric total carbon dioxide analysis for marine studies: maximizing the performance of an automated gas extraction system and coulometric detector. Marine Chemistry, 44, 167-187.

Johnson, KM, Dickson AG, Eischeid G, Goyet C, Guenther P, Key RM, Millero FJ, Purkerson D, Sabine CL, Schottle RG, Wallace DWR, Wilke RJ, Winn CD. (1998). Coulometric total carbon dioxide analysis for marine studies: assessment of the quality of total inorganic carbon measurements made during the US Indian Ocean CO2 Survey 1994-1996. Marine Chemistry. 63, 21-37.

Langdon, C. (2010). Determination of dissolved oxygen in seawater by winkler titration using the amperometric technique. IOCCP Report Nº14, ICPO publication series N 134.

Liu, X., Patsavas, M.C., Byrne, R.H., 2011. Purification and Characterization of meta-Cresol Purple for Spectrophotometric Seawater pH Measurements. Environ. Sci. Technol. 45(11), 4862-8, doi: 10.1021/es200665d.

Margolin A.R., Gonelli, M., Hansell, D., and Santinelli, C. (2018). Black Sea dissolved organic matter dynamics: Insights from optical analyses: Black Sea dissolved organic matter dynamics. Limnol. Oceanogr. doi: 10.1002/lno.10791

Mintrop, L., F. F. Pérez, M. González Dávila, A. Körtzinger and J.M. Santana Casiano (2000). Alkalinity determination by potentiometry- intercalibration using three different methods.CienciasMarinas , 26 , 23-37.

Nelson N.B. and Siegel D.A. (2013). The global distribution and dynamics of chromophoric dissolved organic matter. Annu. Rev. Mar. Sci. 2013.5, 447-476.

Patsavas MC, Byrne RB, Yang B, Easley RA, Wanninkhof R, Liu X (2015). Procedures for direct spectrophotometric determination of carbonate ion concentrations: Measurements in US Gulf of Mexico and East Coast waters. Marine Chemistry, 168, 80-85.

Pérez, F.F. and F. Fraga (1987).A precise and rapid analytical procedure for alkalinity determination. Marine Chemistry, 21, 169-182

Pérez, F.F., A.F. Ríos, T. Rellán and M. Álvarez (2000). Improvements in a fast potentiometric seawater alkalinity determination.Ciencias Marinas, 26, 463-478.

Retelletti Brogi, S., Gonnelli, M., Vestri, S. and Santinelli, C. (2015). Biophysical processes affecting DOM dynamics at the Arno river mouth (Tyrrhenian Sea). Biophysical Chemistry, 197, 1-9.

Santinelli C., Follett C.L., Retelletti Brogi S., Xu L. and Repeta D.J. (2015). Carbon isotope measurements reveal unexpected cycling of dissolved organic matter in the deep Mediterranean Sea. Mar Chem., 177, 267-277.

Santinelli C. (2015). DOC in the Mediterranean Sea. In: Dennis A. Hansell and Craig A. Carlson (eds.) Biogeochemistry of Marine Dissolved Organic Matter, pp. 579-608. Burlington: Academic Press.

Santinelli C., Seritti A. and Nannicini L. (2010). DOC dynamics in the meso and bathypelagic layers of the Mediterranean Sea. Deep-Sea Research **II**, 57, 1446-1459.

Santinelli C., Hansell D. and Ribera D'Alcalà M. (2013). Influence of stratification on marine dissolved organic carbon (DOC) dynamics: The Mediterranean Sea case. Progress in Oceanography 119, 68-77.

Santinelli C., Sempéré R., Van Wambeke F., Charriere B., Seritti A. (2012) Organic carbondynamics in the Mediterranean Sea: An integrated study. Global Biogeochemical Cycles 26, doi:10.1029/2011GB004151.

Sigman, D.M., K.L. Casciotti, M. Andreani, C. Barford, M. Galanter, and J.K. Böhlke. 2001. A bacterial method for the nitrogen isotopic analysis of nitrate in seawater and freshwater. Anal. Chem. 73: 4145-4153.

Stedmon C.A. and Nelson N.B. (2015). The optical properties of DOM in the ocean. Biogeochemistry of Marine Dissolved Organic Matter 2nd Ed., 481-508.

Turnherr, A.M. (2014). How To Process LADCP Data With the LDEO Software (Versions IX.7 – IX.10). The "go-ship" manual for LADCP data acquisition ftp://ftp.ldeo.columbia.edu/pub/LADCP/UserManuals

Ullmann, D. S. and Hebert D. (2014): Processing of Underway CTD data. AMS https://doi.org/10.1175/JTECH-D-13-00200.1

Weigand, M.A., J. Foriel, B. Barnett, S. Oleynik, and D.M. Sigman. 2016. Updates to instrumentation and protocols for isotopic analysis of nitrate by the denitrifier method. Rapid Commun. Mass Spectrom. 30: 1365-1383.

Yao, W., Liu, X., Byrne, R.H., 2007. Impurities in indicators used for spectrophotometric seawater pH measurements: Assessment and remedies. Mar. Chem. 107, 167–172, doi: 10.1016/j.marchem.2007.06.012